THESIS

STRUCTURE AND DYNAMICS OF WATER CONFINED IN SINGLE-WALLED NANOTUBES: A MOLECULAR DYNAMICS STUDY

NONGNUCH ARTRITH

A Thesis Submitted in Partial Fulfillment of
the Requirements for the Degree of
Master of Science (Chemistry)
Graduate School, Kasetsart University
2008

THESIS

STRUCTURE AND DYNAMICS OF WATER CONFINED IN SINGLE-WALLED NANOTUBES: A MOLECULAR DYNAMICS STUDY

NONGNUCH ARTRITH

GRADUATE SCHOOL, KASETSART UNIVERSITY

2008

THESIS APPROVAL

GRADUATE SCHOOL, KASETSART UNIVERSITY

Master of Science (Chemistry)

DEGREE

Chemistry	Chemistry
FIELD	**DEPARTMENT**

TITLE: Structure and Dynamics of Water Confined in Single-Walled Nanotubes: A Molecular Dynamics Study

NAME: Miss Nongnuch Artrith

THIS THESIS HAS BEEN ACCEPTED BY

..... **THESIS ADVISOR**

(Assistant Professor Piboon Pantu, Ph.D.)

..... **COMMITTEE MEMBER**

(Professor Jumras Limtrakul, Ph.D.)

..... **COMMITTEE MEMBER**

(Mr. Tanin Nanok, Ph.D.)

..... **DEPARTMENT HEAD**

(Associate Professor Noojaree Prasitpan, Ph.D.)

APPROVED BY THE GRADUATE SCHOOL ON .....

..... **DEAN**

(Associate Professor Vinai Artkongharn, M.A.)

Nongnuch Artrith 2008: Structure and Dynamics of Water Confined in Single-Walled Nanotubes: A Molecular Dynamics Study. Master of Science (Chemistry), Major Field: Chemistry, Department of Chemistry. Thesis Advisor: Assistant Professor Piboon Pantu, Ph.D. 78 pages.

Structures and dynamics of water molecules in nanoporous media exhibit interesting characteristics different from their ordinary bulk properties and may lead to potential applications in sophisticated nanofludic devices. In this study, molecular dynamics simulations were performed to investigate water molecules confined in single-walled carbon nanotubes (SWCNTs) and boron nitride nanotubes (SWBNNTs). Water density of 1.00 g cm^{-3} was placed inside the models of (*n*,*n*)-armchair nanotubes with different diameterrs (*n* = 9, 10, 12, 14, 16 and 20) and the simulations were performed in the canonical *NVT* ensemble at 298 K by using the Nosé-Hoover thermostat in DL_POLY program package. The wall-water interactions were varied within reasonable limits by changing the strength of the Lennard-Jones (LJ) parameters. Distribution functions were reported for the water in the tubes in spherical and cylindrical coordinates and the single-molecule dynamics, in particular self-diffusion, were monitored. While this motion was very much slowed down in narrow tubes, in keeping with previous findings (Mashl, R.J. *et al*. 2003 Nano Lett. 3(5):589-592.), bulk-water like self-diffusion coefficients were found in wider tubes. Axial diffusion coefficient increased with increasing tube diameter and reached its bulk value in the widest tubes with diameters of about 24 Å. The convergence was faster for smaller wall-water interactions. An anomaly is, however, found for the SWBNNTs where the convergence was not monotonous.

_____ _____ ___ / ___ / ___

Student's signature Thesis Advisor's signature

ACKNOWLEDGEMENT

This thesis would not have been complete at all without the help and support by many people. I wish to express my deep gratitude to whom giving me the guidance to reach my goal of this study. First of all, most of credits in this should justifiably go to Department of Chemistry, Kasetsart University and my advisors; Professor Dr. Jumras Limtrakul and Assistant Professor Dr. Piboon Pantu, for the chance to work on a challenging project in a very nice, continuous support, kindness and encouragement during the course of my graduate. I am deeply appreciated and special thanks to Dr. Tanin Nanok who always took the time to help and taught me how chemistry and physics really work together. I could not have imagined having a better advisor and mentor for my study. He forever provides me for precious supervision, considerably helpful comments and discussion on various aspects to my research work.

Furthermore, I would like to thank my entire Physical Chemist teachers, Associate Professor Supa Hannongbua, Dr. Pensri Boonsawansong Dr. Chack Sangma, for their basic knowledge of Physical Chemistry and suggestions. Special thanks are due to Professor Philippe Anthony Bopp (Laboratoire de Physico-Chimie Moléculaire, Université Bordeaux I and CNRS (UMR 5803), F-33405, Talence CEDEX, France) for his programming valuable assistance was very nice and continuing supports in various ways.

This work was supported in part by grants from the Thailand Research Fund and the Kasetsart University Research and Development Institute (KURDI), the National Nanotechnology Center (NANOTEC center of Excellence and Computational Nanoscience Consortium), the National Research Council of Thailand (NRCT) and the Commission on Higher Education (Postgraduate Education and Research Programs in Petroleum, and Petrochemicals, and Advanced Materials and Postdoctoral Research Grants to TN), Ministry of Education. The support from the Graduate School Kasetsart University is also acknowledged.

My colleagues at Laboratory for Computational and Applied Chemistry (LCAC) at Kasetsart University are sincerely thanked for their considerable helpful assistance during my study; Miss Boonruen Sunpetch, Mr. Boondej Boekfah and Mr. Chadchalerm Raksakool. In addition, all of my friends are honestly grateful for their supporting and sharing useful ideas.

Finally, I would like to give my most profound thankfulness to my parents and my sister for their love, truthful care and great encouragement throughout the duration of my educations.

Nongnuch Artrith
March 2008

TABLE OF CONTENTS

LIST OF TABLES

LIST OF FIGURES

LIST OF FIGURES (Continued)

LIST OF FIGURES (Continued)

LIST OF ABBREVIATIONS

Dz	=	Self-diffusion coefficient (z axis)
BLYP	=	Beck-Lee-Yang-Parr functional
BN	=	Boron nitride
BNNTs	=	Boron nitride nanotubes
CNTs	=	Carbon nanotubes
GlpF	=	Glycerol the crystal structure (F is symbol of native glycerol)
HF	=	Hartree-Fock
Ix	=	Angular momentum x component
Iy	=	Angular momentum y component
Iz	=	Angular momentum z component
LJ	=	Lennard-Jones
MC	=	Monte Carlo
MD	=	Molecular dynamics
MSD	=	Mean square displacement
MWCNT	=	Multi walled carbon nanotube
n(r)	=	Coordination number
NPT	=	Isothermal-Isobaric (NPT) ensemble
NT	=	Nanotubes
NVE	=	Microcanonical ensemble (NVE)
NVT	=	Canonical ensemble (NVT)
PW	=	Plane-Wave
RDF	=	Radial distribution function
SPC	=	Simple point charge
SPC/E	=	Extended simple point charge
STM	=	Temperature scanning tunneling microscope
SWBNNT	=	Single walled boron nitride nanotube
SWCNT	=	Single walled carbon nanotube
TEM	=	Transmission electron microscopy

TABLE OF CONTENTS

LIST OF TABLES

LIST OF FIGURES

LIST OF FIGURES (Continued)

LIST OF FIGURES (Continued)

LIST OF ABBREVIATIONS

Dz	=	Self-diffusion coefficient (z axis)
BLYP	=	Beck-Lee-Yang-Parr functional
BN	=	Boron nitride
BNNTs	=	Boron nitride nanotubes
CNTs	=	Carbon nanotubes
GlpF	=	Glycerol the crystal structure (F is symbol of native glycerol)
HF	=	Hartree-Fock
Ix	=	Angular momentum x component
Iy	=	Angular momentum y component
Iz	=	Angular momentum z component
LJ	=	Lennard-Jones
MC	=	Monte Carlo
MD	=	Molecular dynamics
MSD	=	Mean square displacement
MWCNT	=	Multi walled carbon nanotube
n(r)	=	Coordination number
NPT	=	Isothermal-Isobaric (NPT) ensemble
NT	=	Nanotubes
NVE	=	Microcanonical ensemble (NVE)
NVT	=	Canonical ensemble (NVT)
PW	=	Plane-Wave
RDF	=	Radial distribution function
SPC	=	Simple point charge
SPC/E	=	Extended simple point charge
STM	=	Temperature scanning tunneling microscope
SWBNNT	=	Single walled boron nitride nanotube
SWCNT	=	Single walled carbon nanotube
TEM	=	Transmission electron microscopy

THESIS

STRUCTURE AND DYNAMICS OF WATER CONFINED IN SINGLE-WALLED NANOTUBES: A MOLECULAR DYNAMICS STUDY

NONGNUCH ARTRITH

A Thesis Submitted in Partial Fulfillment of
the Requirements for the Degree of
Master of Science (Chemistry)
Graduate School, Kasetsart University
2008

THESIS

STRUCTURE AND DYNAMICS OF WATER CONFINED IN SINGLE-WALLED NANOTUBES: A MOLECULAR DYNAMICS STUDY

NONGNUCH ARTRITH

GRADUATE SCHOOL, KASETSART UNIVERSITY

2008

THESIS APPROVAL

GRADUATE SCHOOL, KASETSART UNIVERSITY

Master of Science (Chemistry)

DEGREE

Chemistry	Chemistry
FIELD	**DEPARTMENT**

TITLE: Structure and Dynamics of Water Confined in Single-Walled Nanotubes: A Molecular Dynamics Study

NAME: Miss Nongnuch Artrith

THIS THESIS HAS BEEN ACCEPTED BY

..... **THESIS ADVISOR**

(Assistant Professor Piboon Pantu, Ph.D.)

..... **COMMITTEE MEMBER**

(Professor Jumras Limtrakul, Ph.D.)

..... **COMMITTEE MEMBER**

(Mr. Tanin Nanok, Ph.D.)

..... **DEPARTMENT HEAD**

(Associate Professor Noojaree Prasitpan, Ph.D.)

APPROVED BY THE GRADUATE SCHOOL ON .....

..... **DEAN**

(Associate Professor Vinai Artkongharn, M.A.)

Nongnuch Artrith 2008: Structure and Dynamics of Water Confined in Single-Walled Nanotubes: A Molecular Dynamics Study. Master of Science (Chemistry), Major Field: Chemistry, Department of Chemistry. Thesis Advisor: Assistant Professor Piboon Pantu, Ph.D. 78 pages.

Structures and dynamics of water molecules in nanoporous media exhibit interesting characteristics different from their ordinary bulk properties and may lead to potential applications in sophisticated nanofludic devices. In this study, molecular dynamics simulations were performed to investigate water molecules confined in single-walled carbon nanotubes (SWCNTs) and boron nitride nanotubes (SWBNNTs). Water density of 1.00 g cm^{-3} was placed inside the models of (*n*,*n*)-armchair nanotubes with different diameterrs (*n* = 9, 10, 12, 14, 16 and 20) and the simulations were performed in the canonical *NVT* ensemble at 298 K by using the Nosé-Hoover thermostat in DL_POLY program package. The wall-water interactions were varied within reasonable limits by changing the strength of the Lennard-Jones (LJ) parameters. Distribution functions were reported for the water in the tubes in spherical and cylindrical coordinates and the single-molecule dynamics, in particular self-diffusion, were monitored. While this motion was very much slowed down in narrow tubes, in keeping with previous findings (Mashl, R.J. *et al*. 2003 Nano Lett. 3(5):589-592.), bulk-water like self-diffusion coefficients were found in wider tubes. Axial diffusion coefficient increased with increasing tube diameter and reached its bulk value in the widest tubes with diameters of about 24 Å. The convergence was faster for smaller wall-water interactions. An anomaly is, however, found for the SWBNNTs where the convergence was not monotonous.

_____ _____ ___ / ___ / ___

Student's signature Thesis Advisor's signature

ACKNOWLEDGEMENT

This thesis would not have been complete at all without the help and support by many people. I wish to express my deep gratitude to whom giving me the guidance to reach my goal of this study. First of all, most of credits in this should justifiably go to Department of Chemistry, Kasetsart University and my advisors; Professor Dr. Jumras Limtrakul and Assistant Professor Dr. Piboon Pantu, for the chance to work on a challenging project in a very nice, continuous support, kindness and encouragement during the course of my graduate. I am deeply appreciated and special thanks to Dr. Tanin Nanok who always took the time to help and taught me how chemistry and physics really work together. I could not have imagined having a better advisor and mentor for my study. He forever provides me for precious supervision, considerably helpful comments and discussion on various aspects to my research work.

Furthermore, I would like to thank my entire Physical Chemist teachers, Associate Professor Supa Hannongbua, Dr. Pensri Boonsawansong Dr. Chack Sangma, for their basic knowledge of Physical Chemistry and suggestions. Special thanks are due to Professor Philippe Anthony Bopp (Laboratoire de Physico-Chimie Moléculaire, Université Bordeaux I and CNRS (UMR 5803), F-33405, Talence CEDEX, France) for his programming valuable assistance was very nice and continuing supports in various ways.

This work was supported in part by grants from the Thailand Research Fund and the Kasetsart University Research and Development Institute (KURDI), the National Nanotechnology Center (NANOTEC center of Excellence and Computational Nanoscience Consortium), the National Research Council of Thailand (NRCT) and the Commission on Higher Education (Postgraduate Education and Research Programs in Petroleum, and Petrochemicals, and Advanced Materials and Postdoctoral Research Grants to TN), Ministry of Education. The support from the Graduate School Kasetsart University is also acknowledged.

My colleagues at Laboratory for Computational and Applied Chemistry (LCAC) at Kasetsart University are sincerely thanked for their considerable helpful assistance during my study; Miss Boonruen Sunpetch, Mr. Boondej Boekfah and Mr. Chadchalerm Raksakool. In addition, all of my friends are honestly grateful for their supporting and sharing useful ideas.

Finally, I would like to give my most profound thankfulness to my parents and my sister for their love, truthful care and great encouragement throughout the duration of my educations.

Nongnuch Artrith
March 2008

TABLE OF CONTENTS

LIST OF TABLES

LIST OF FIGURES

LIST OF FIGURES (Continued)

LIST OF FIGURES (Continued)

LIST OF ABBREVIATIONS

Dz	=	Self-diffusion coefficient (z axis)
BLYP	=	Beck-Lee-Yang-Parr functional
BN	=	Boron nitride
BNNTs	=	Boron nitride nanotubes
CNTs	=	Carbon nanotubes
GlpF	=	Glycerol the crystal structure (F is symbol of native glycerol)
HF	=	Hartree-Fock
Ix	=	Angular momentum x component
Iy	=	Angular momentum y component
Iz	=	Angular momentum z component
LJ	=	Lennard-Jones
MC	=	Monte Carlo
MD	=	Molecular dynamics
MSD	=	Mean square displacement
MWCNT	=	Multi walled carbon nanotube
n(r)	=	Coordination number
NPT	=	Isothermal-Isobaric (NPT) ensemble
NT	=	Nanotubes
NVE	=	Microcanonical ensemble (NVE)
NVT	=	Canonical ensemble (NVT)
PW	=	Plane-Wave
RDF	=	Radial distribution function
SPC	=	Simple point charge
SPC/E	=	Extended simple point charge
STM	=	Temperature scanning tunneling microscope
SWBNNT	=	Single walled boron nitride nanotube
SWCNT	=	Single walled carbon nanotube
TEM	=	Transmission electron microscopy

STRUCTURE AND DYNAMICS OF WATER CONFINED IN SINGLE-WALLED NANOTUBES: A MOLECULAR DYNAMICS STUDY

INTRODUCTION

Carbon nanotubes (CNTs) (Iijima, 1991) have gained recognition as prominent building blocks of nano-materials. Due to their exceptional mechanical and electrical properties, several potential applications have been proposed such as nanoelectronic devices, composite materials, molecular sieves/membrane separation, nanofluidic devices, etc. (Meyyappan, 2005). The transport of molecules in these nanoporous media exhibits interesting characteristics, different from those of transport in ordinary bulk media (Behler *et al.*, 2001; Hummer *et al.*, 2001), since the interactions between the pore wall and molecules become rather strong when the dimensions of the pore approach the size of the transported molecule (Hummer *et al.*, 2001). Although the mechanical and electrical properties of CNTs can be measured explicitly by experiments (Wang *et al.*, 2000), the understanding on transport and conduction mechanisms through their pores is still uncertain. This is partly due to the difficulty of preparing CNTs with uniform pore sizes and distributions and of tracing diffusive behaviors of molecules inside nanopores. Computational studies, thus, play an important role in the interpretation of experimental data and provide predictive information on molecular transport through nanopores.

Because of the simplicity and hydrophobicity of their interior, CNTs are recognized as promising prototype models. They are frequently used as models for systems such as water transport in aquaporin water channels (Sui *et al.*, 2001), water migration in xylem vessels of plants (Kolesnikov *et al.*, 2004) and the delivery of beneficial molecules to the target cells (Bianco *et al.*, 2005; Chou *et al.*, 2008; Tajkhorshid *et al.*, 2002) and other biological nano-fluidic systems.

A previous molecular dynamics (MD) simulation study (Hummer *et al.*, 2001) on water conduction through the channel of single-walled carbon nanotubes (SWCNTs) showed that under normal conditions of pressure and temperature the filling of an empty (6,6)-CNT channel (8.1 Å in diameter and 13.4 Å in length) with water takes place within a few ten picoseconds. The channel then remained filled during the entire simulation time of 66 ns. The water molecules constrained in such a narrow space form a one-dimensionally ordered hydrogen-bond network that is not observed in bulk water. It was shown that the channel occupancy and conductivity are dramatically decreased by a reduction of the attractive nanotube–water interactions. A 25% reduction (Waghe *et al.*, 2002) leads to fluctuations between filled and empty sections in the tube and a 40% reduction to an emptying of the CNT channel (Hummer *et al.*, 2001). The filling and conducting behavior has also been observed in an isoelectronic nanotube (a subnanometer boron nitride nanotube (BNNT) (Won and Aluru, 2007)) and other hydrophobic nanopores (Joseph and Aluru, 2008; Noy *et al.*, 2007; Won and Aluru, 2008).

Recently, several MD simulation studies have been performed on the diameter dependence of the CNT hydration. It was found that water confined in a critical-size armchair-(9,9) CNT can undergo a transition into a state having ice-like mobility with a average number of hydrogen bonds close to that in bulk water under ambient temperature and pressure (Mashl *et al.*, 2003). Unusual features, not seen in bulk ice, can also be observed with other CNT diameters under conditions of high water densities (Liu *et al.*, 2005a; Mashl *et al.*, 2003) and extremely high axial pressures (50 Mpa to 500 Mpa) (Koga *et al.*, 2000). The radial distribution functions reveal highly ordered layer water structures of water in this case. For the dynamic properties, the radial and axial diffusivity of water encapsulated in SWCNTs are smaller than that the bulk water diffusivity; both decrease as the diameter of SWCNTs decreases (Koga *et al.*, 2000; Liu and Wang, 2007; Liu and Consta, 2005; Liu and Wang, 2005; Liu *et al.*, 2005a; Liu *et al.*, 2005b). In other tubes with similar diameters, the flow of water was found to be strongly influenced by the

hydrophilicity of the wall. The strong interfacial water-nanotube attraction causes a significant reduction of the water flow rate.

Even though the structure and dynamics of water confined in SWCNTs have been extensively studied by MD simulations, most efforts have been directed toward small diameter tubes, in which the characteristics of bulk water at the tube center will never be attained. Thus, a more comprehensive understanding of the structural and dynamic properties of confined water in larger diameter SWCNTs remains to be unraveled. Here, this research studies tubes with effective diameters between 8.86 to 23.74 Å and report on the influences of the attractive interactions between the water and the wall on structural and dynamic properties of confined water at average density of 1.00 g cm^{-3} under ambient conditions.

In the next section, the models and simulation details will be presented. Then, this work will investigate the structure of the water in the tubes in terms of radial and spherical distribution functions. A detailed study of the self-diffusion will then be presented.

LITERATURE REVIEW

Sumio Iijima discovered a novel carbon allotrope carbon tubule, formed by a high current arc discharge process to evaporate graphite (Iijima, 1991; Iijima *et al*., 1993). The small tubes consisted of layer tube-like graphene structures, each succeeding outer shell having a larger diameter. These tubules were called multi-walled carbon nanotubes (MWCNTs). Carbon nanotubes consist of a shell of sp^2-hybridized carbon atoms forming a hexagonal network similar to a graphene sheet, which has been rolled up into a cylindrical shape.

The single-shelled nanotube, made up of a single layer of carbon atoms was called single-walled carbon nanotube (SWCNT) (Iijima *et al*., 1993). A typical SWCNT will have a cylindrical structure with diameter in the order of nanometers and can be a few micrometers long. SWCNT should be at least 0.4 nm large to afford strain energy and at most about 3.0 nm large to maintain tubular structure and prevent collapsing. Typical experimentally observed SWCNT is between 0.6 to 2.0 while smaller (0.4 nm) and large (3.0 nm) SWCNTs have been reported (Wang *et. al*., 2000). A larger SWCNT tends to collapse unless it is supported by force or surrounded by neighboring tubes, such as in a MWCNT. Typically MWCNT diameter is larger than 2.0 nm inside and smaller than 100 nm outside see the example of MWCNT in Figure 1. A SWCNT rope is formed usually through a self-organization process in which van der Waals force holds individual SWCNT together to form a triangle lattice with lattice constant of 0.34 nm (Meyyappan, 2005).

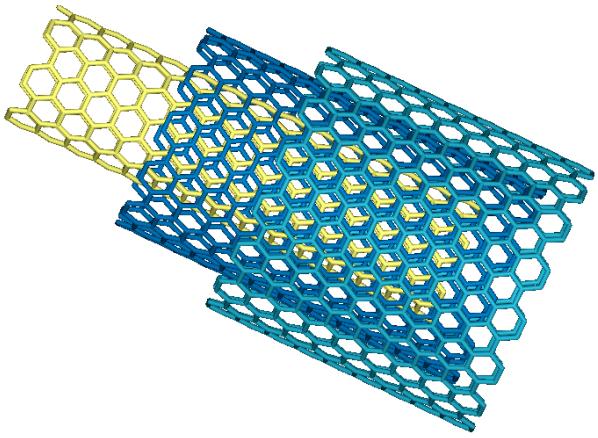

(a)

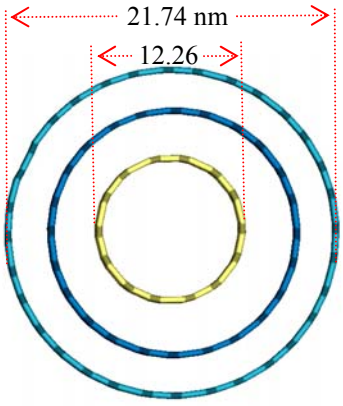

(b)

Figure 1 Multi-walled carbon nanotubes (MWCNTs) structures: 3 layers model of side view MWCNTs **(a)** and 3 layers model of top view MWCNTs **(b)**; diameter of (9,9)-CNT (smallest tube), (12,12)-CNT (middle tube) and (16,16)-CNT (biggest tube).

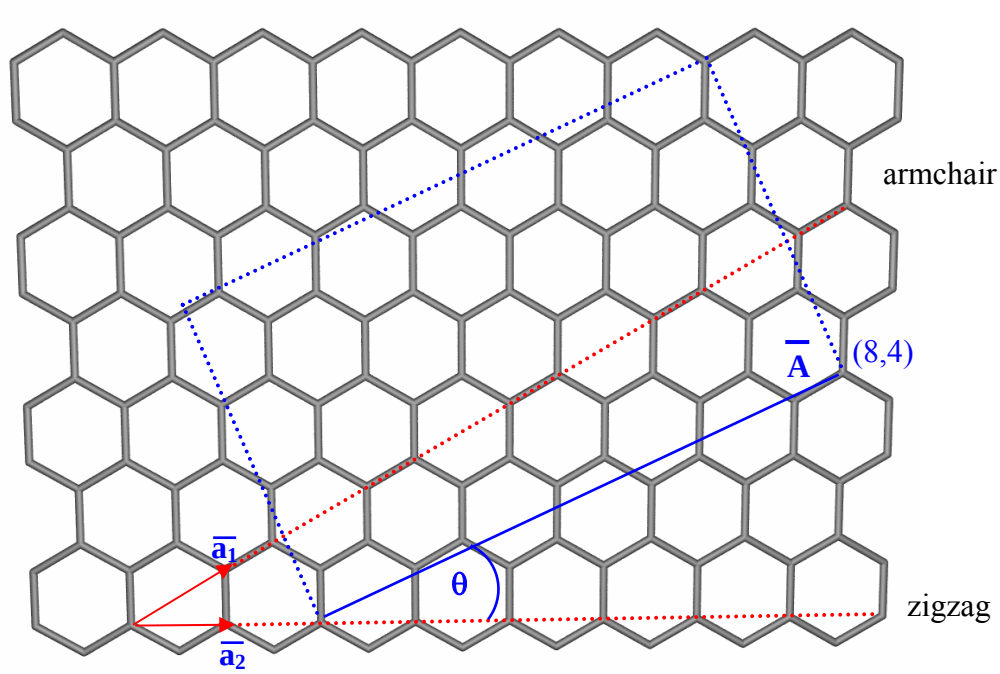

Figure 2 Carbon nanotube (n,m) is formed by rolling a graphite sheet along the chiral vector $\mathbf{A} = n\mathbf{a}_1 + m\mathbf{a}_2$ on the graphite where $\mathbf{a}_1$ and $\mathbf{a}_2$ are graphite lattice vector; m and n are integers.

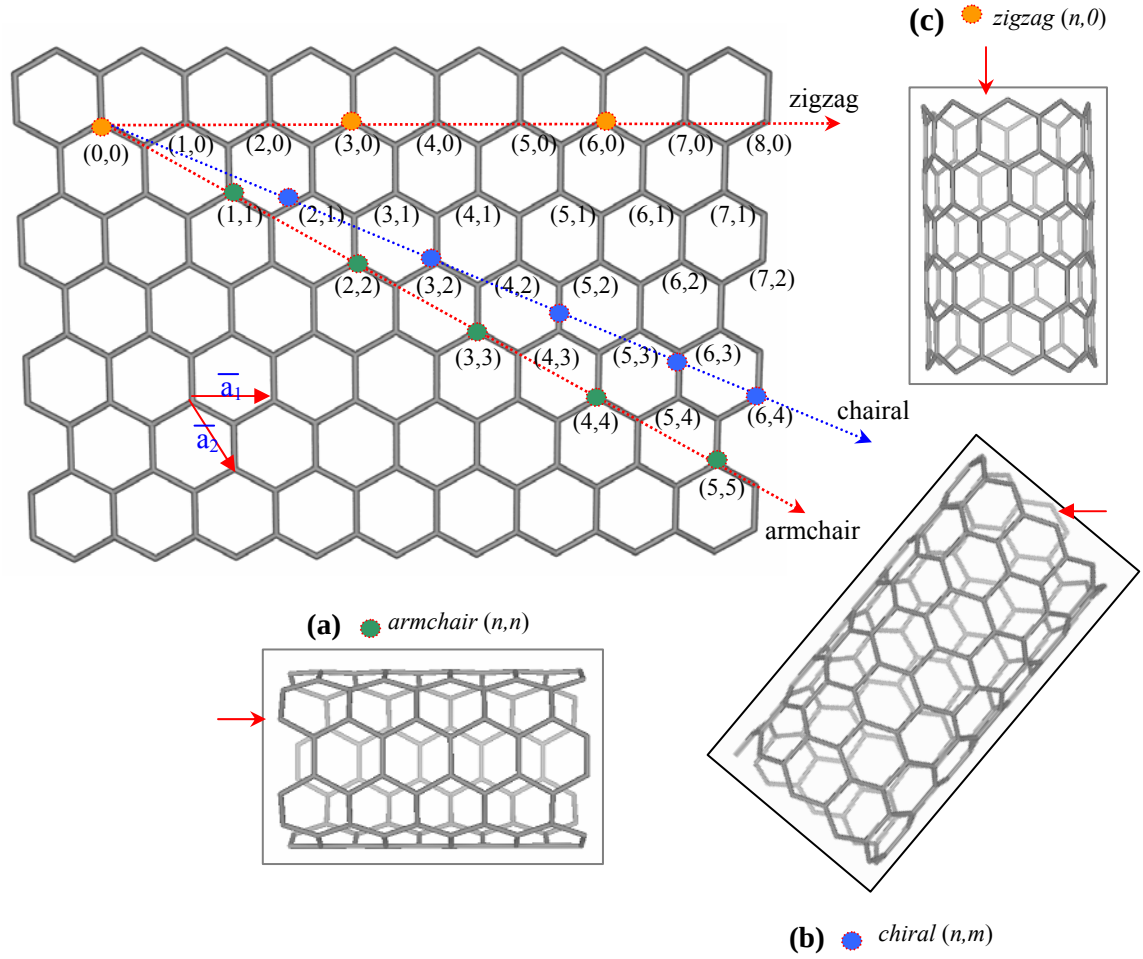

Figure 3 Single-walled carbon nanotubes (SWCNTs) by rolling a graphene sheet in different chirality: armchair (*n,n*)**(a)**; chiral (*n,m*)**(b)**; zigzag (*n,0*)**(c)**. In the example, they are (5,5), (6,4) and (8,0) nanotubes.

Single wall carbon nanotube (SWCNT) can be viewed as a single sheet of graphite that has been rolled up along the chiral vector **A**, which can be characterized by the diameter and the chiral angle θ (see Figure 2).

$$\mathbf{A} = n\mathbf{a}_1 + m\mathbf{a}_2 \qquad (1)$$

where $\mathbf{a}_1$ and $\mathbf{a}_2$ are unit vectors of the hexagonal honeycomb lattice and n and m are integers. This chiral vector **A** also defines a chiral angle, θ which is the angle between **A** and the zigzag direction of the graphene sheet. All nanotube's type is usually characterized by these two integer numbers (n,m), such as *armchair* (n,n) and *zigzag* (n,0) or *chiral* (n,m) classes (see Figure 3). The electronic properties of nanotubes can be metallic and semiconductor and follow a general rule: all armchair SWCNTs are metals; those with $n - m = 3i$, where i is a nonzero integer, are semiconductors with a small band gap; and all others are semiconductors with a band gap that inversely depends on the nanotubes diameter (Saito *et al.,* 1992).

Despite their simple chemical composition and atomic bonding configuration, carbon nanotubes (CNTs) exhibit a great variety in structures and structure–property relations. CNTs exhibit rather outstanding and unique mechanical and physical properties, and immediately after their discovery were regarded as new materials for future technologies. In the present they are widely known as the necessary contributors to nano-technology, a technology concerned with the control and practice of matter on the nanometer to molecular scale and with the creation of nanoscale building blocks with fundamentally new physical, chemical, biological properties and functions. Their great progress has been made toward many applications for example; chemical and biological separation, energy storage, composite materials, probes, sensors and actuators for molecular imaging, sensing and manipulation, transistors, memories, logic devices, field emission devices, flat panel display and other nanoelectronic devices (Meyyappan, 2005). The advantages of these applications have been demonstrated, including their small size,

low power, and low weight. These applications and advantages can be understood by the unique structure and properties of nanotubes.

Diffusion and molecular distribution of simple and complex fluid in carbon nanotubes are important as of both fundamental science and applications (Kalra *et al.*, 2003; Kalra *et al.*, 2004; Supple and Quirke, 2003; , 2004; , 2005). The motivation to study of water confined in CNTs, because of they have gained much attention as prototypes for biological water channels due to their simplicity, stability, and nanoporosity. This basic knowledge has led to development of theoretical predictions of the availability of carbon-nanotube-based membranes will permit the experimental verification. Understanding the mechanism of water diffusion under this condition, the goal of this contribution, is crucial for designing novel nanomachine such as water channel in biosystem, nanosyringes and synthetic nanomembranes for the controlled delivery of nanometer quantities of aqueous solutions.

CNTs are recognized as promising prototype models. They are frequently used as models for systems; water transport in aquaporin water channels (Sui *et al.*, 2001), water channels facilitate the rapid transport of water across cell membranes in response to osmotic gradients. These channels were believed to be involved in many physiological processes that included renal water conservation, neuro-homeostasis, digestion, regulation of body temperature and reproduction. Additionally, water migration in xylem vessels of plants, the delivery of beneficial molecules to the target cells (Tajkhorshid *et al.*, 2002) and other biological nano-fluidic systems are also interesting for modeled.

Following their discovery, carbon nanotubes have attracted interest because of their unusual electrical and mechanical properties, and their hollow interior that can serve as a nanometre-sized conduit, or template in material fabrication. The ability to encapsulate a material in a nanotube also offers new possibilities for investigating dimensionally confined phase transitions. Matter within the narrow confines of a carbon nanotube might exhibit a solid-liquid critical point beyond which the distinction between solid and liquid phases disappears (Koga and Tanaka, 2005; Koga *et al.*, 2000). This unusual feature, which cannot occur in bulk material, would allow for the direct and continuous transformation of liquid matter into a solid. CNTs have emerged as a new alternative and efficient tool for transporting and translocating therapeutic molecules. CNTs can be functionalized with bioactive peptides, proteins, nucleic acids and drug, and used to deliver their cargos to cells and organs, because functionalized CNTs display low toxicity and they are not immunogenic, such systems hold great potential in the field of nanobiotechnology and nanomedicine (Bianco *et al.*, 2005).

In 2001, Hummer and *et al*. studied the system of (6,6)-armchair SWCNT put in water bath and reported that confinement of matter on the nanometer scale could induce phase transitions not seen in bulk systems (Hummer *et al*, 2001). In case of water, so-called drying transitions occur on this scale as a result of strong hydrogen bonding between water molecules. The molecular dynamics simulations showed spontaneous and continuous filling of a nonpolar carbon nanotube with a one-dimensionally ordered chain of water molecules. The observations revealed pulse-like transmission of water through the nanotube. These transmission bursts resulted from the tight hydrogen-bonding network inside the tube. The attraction between the tube wall and water dramatically affects pore hydration, leading to sharp, two-state transitions between empty and filled states on a nanosecond timescale. That work suggested that carbon nanotubes, with their rigid nonpolar structures, might be exploited as unique molecular channels for water and protons. The channel occupancy and conductivity may be tunable by changes in the local channel polarity and solvent conditions.

Recently, many MD simulation studies have performed on the diameter dependence of the CNT hydration. By varying CNT diameter, it is found that water confined in a critical-size armchair-(9,9) CNT can undergo transition into a state having ice-like mobility with a number of hydrogen bonds close to that in bulk water under ambient temperature and pressure (Mashl *et al.*, 2003). The unusual features unseen in bulk ice can also be observed in other diameters of CNT under conditions of high water densities (Liu *et al.*, 2005a) and of extremely high axial pressures (50 Mpa to 500 Mpa) (Bai *et al.*, 2006; Koga *et al.*, 2000). The radial distribution functions reveal highly ordered layer structures of water confined in CNTs. For the dynamic properties, the radial and axial diffusivity of water encapsulated in SWCNTs are smaller than that in bulk water and decrease as the diameter of SWCNTs decreases (Liu and Wang, 2005; Liu *et al.*, 2005a; Liu *et al.*, 2005b; Mashl *et al.*, 2003; Striolo, 2006; Striolo *et al.*, 2003; , 2006). With a similar size in diameter, the flow of water in nanotubes is strongly influenced by the hydrophilicity of the nanotube wall. The strong interfacial water-nanotube attraction causes the reduction of the water flow rate significantly (Joseph and Aluru, 2008). Although the structure and dynamics of water confined in SWCNTs have been extensively studied using MD simulations, much effort has been mainly paid on small diameter nanotubes in which the characteristic of bulk water at the tube center will never been attained.

A new anomalously immobilized water phase induced by confinedment in nanotubes was reported by Mashl *et al*, 2003. The MD simulations showed that water confined in CNTs of a critical size (8.6 Å Van der Waals diameter nanotube) under ambient conditions (1 bar, 300 K) had anomalouse icelike behaviors. Moreover, because of a variety of evidence suggesting that water ordering may modulate proton conductance via a proton wire; hydrogen bonding network, the ability to modulate water ordering with geometry suggested a possible mechanism for a switchable nanoscale semiconductor. Also, to study the water alignment and proton conduction inside CNTs, first-principles

molecular dynamics simulations have been carried out to investigate the structure, electronic properties, and proton conductivity of water confined inside single-walled carbon nanotubes (Mann and Halls, 2003). The simulations predict the formation of a strongly connected one-dimensional hydrogen-bonded water wire resulting in a net electric dipole moment directed along the nanotube axis. An excess proton injected into the water wire has found to be significantly stabilized, relative to the gas phase, due to the high polarizability of the carbon nanotube.

Molecular distribution and dynamic properties of confined water were most studied. Temperature effects on the static and dynamic properties of liquid water inside carbon nanotubes were studied by Marti and Gordillo (Marti and Gordillo, 2001a; 2001b; , 2002; , 2003). They reported a series of MD simulation of the behavior of SPC liquid water adsorbed in carbon nanotubes under different thermodynamics. A flexible simple point charged potential was employed to model internal and intermolecular water interactions. System was radii ranging from 4.1 Å to 6.8 Å and three temperatures from 298 K to 500 K for density of 1.00 g cm^{-3}. Results showed the gradual destruction of the hydrogen-bond network together with faster diffusive regimes as temperature increases. The vibrational mode absent in bulk-unconstrained water appeared in the power spectra obtained from hydrogen velocity autocorrelation functions for all thermodynamic states. That frequency mode attributed to confinement effects. Diffusive behavior and the vibrational, rotational, intra- and intermolecular motions of the constrained molecules were investigated by means of the spectral densities computed from atomic velocity autocorrelation functions. The results showed new vibrational bands and frequency shifts that were not observed in bulk water. Other system studied, Marti and Gordillo chose to model water-water and water-carbon forces, respectively. It showed that system underwent a first-order phase transition between low- and high-density phases.

A similar research of the role of transport phenomena of confined water has explored the osmotically driven transport of water molecules through hexagonally packed CNT membranes. Simulation set up two types such semipermeable membranes separate compartments of pure water and salt solution (Kalra *et al.*, 2003). The resulted flow rates were high (average 5.8 water molecules per ns and nanotube, comparable to those through the trans-membrane protein aquaporin-one), and were practically independent of the length of the nanotube, in contrast to predictions of macroscopic hydrodynamics. All of these distinct characteristics of nanoscopic water flow modeled by one-dimensional continuous-time random walk. At long times, they reported that the pure water compartment drained, and the net flow of water interrupted by the formation of structured solvation layers of water sandwiched between two nanotube membranes.

Liu and coworkers published 4 papers in 2005 reported behaviors of water confined in SWCNTs based on MD simulation (Liu and Consta, 2005; Liu and Wang, 2005; Liu *et al.*, 2005a; Liu *et al.*, 2005b). They summarized the investigation of the molecular distribution and transport properties (self-diffusion coefficient, thermal conductivity, and viscosity) of water confined in SWCNT with diameter from 11 Å to 21 Å. Many conditions have been taken in their work such as difference pore sizes, nanotube helicity, and variance density of water and thermal conductivity. For molecular distributions, the water molecules ordered in helix inside the (10, 10) SWCNT. It was also found that the axial thermal conductivity and shear viscosity in SWCNTs were greater than those of the bulk and self-diffusion coefficients of water in the order of armchair CNTs have higher than in zigzag CNTs (Liu and Wang, 2005). Moreover, they pointed that the axial diffusion coefficient was lower than that characteristic of bulk water and that it had decreased as the pore diameter narrows. For the largest nanotube considered (21 Å in diameter), the calculated diffusion coefficient equaled 0.9423×10^{-5} cm^2 s^{-1}. It should however be pointed out that Fickian motion only occurs when the molecules pass each other uncontrollably in the direction of flow. For diffusivity, results showed in model nanotube (fitting curve of NT) > in armchair CNT > in zigzag CNT at

similar conditions. However in contrast to the diffusivity, the thermal conductivity and the shear viscosity have increased as the pore size decreases, in zigzag CNT > in armchair CNT > in model NT. The ordered layer distribution of water molecules in nanotubes was clear. It suggested the structure of fluid in the zigzag CNTs was more ordered, and more solidlike. In the nanotubes, where the molecule and the pore dimensions were of similar order of magnitude, the nature of water-water and water-wall interactions, the confinement effect of space, and the helicity of CNT become more significant.

However, Striolo (Striolo, 2006) mentioned a work of Liu and Wang (Liu and Wang, 2005) that may not be true when fluid molecules were confined in long and narrow nanotubes. Striolo reported the confined water diffuse thought in narrow SWCNT, which occurred via a coordinated motion, and the mean square displacement (MSD) followed as a ballistic-type dependence on time for up to hundreds of picoseconds. As same as previous work, they observed the layered ice-like structures of water confined in SWCNT (Striolo, 2006; Striolo *et al.*, 2003; , 2006; Striolo *et al.*, 2004a; Striolo *et al.*, 2004b). Basic study of those researches would like to use theoretical predictions of the availability of carbon-nanotube-based membranes will permit the experimental verification. Understanding the mechanism of water diffusion under this condition, the goal of this contribution, is crucial for designing nano-machine, nano-injector and synthetic membranes as well as for the development of novel drug-delivery devices.

The filling and ordering properties of water restrained in MWCNTs are also interesting. SWCNTs with different diameters, lengths, and chiralities, could coaxially self-assemble into MWCNTs in water via spontaneous insertion of smaller tubes into larger ones (Zou *et al.*, 2006a; 2006b). The assembly process was tube-size-dependent, and the driving force was primarily the intertube van der Waals interactions. The simulations also suggested that a MWCNT might be separated into SWCNTs under appropriate solvent conditions. Their study proposed possible bottom-up self-assembly routes for the fabrication of novel nanodevices and systems.

The structures of water confined in carbon nanotubes were found to be *n*-gonal ice nanotubes and may be called filled ice nanotubes. In very small tubes (effective diameter of 6-8 Å), water formed a single file ice nanotube (Hummer *et al*, 2001; Marshl *et al*., 2003; Gordillo *et al*., 2000; Gordillo *et al*., 2001). In the critical size tubes (effective diameter of 8-12 Å), one-gonal ice nanotube and in the large tubes (effective diameter up to 12 Å), multi-gonal ice nanotubes were formed (Bai *et al.*, 2006; Li *et al.*, 2007; Li *et al.*, 2006; Takaiwa *et al.*, 2007; Yang and Garde, 2007). Spontaneous formation of the filled ice nanotubes was observed in MD simulations of water at fixed densities and a fixed temperature. Outer-layered filled ice nanotubes characterized by a roll-up vector (*n, m*), while inner files of molecules did not have definite ordered structures. With this notation the filled ice nanotubes are of (*n, n*), (*n, 0*) and (*n, m*) types, the last of which has a helical structure in its outer layer whereas the outer layers of first of two structures as the *n*-gonal ice nanotubes. Structure analysis was done for their hydrogen-bond networks and advanced dipole moments.

Behavior of water encapsulated in carbon nanotubes recommended the existence of a variety of new ice phases not seen in bulk ice, and of a solid-liquid critical point (Koga *et al.*, 2001). Using carbon nanotubes with diameters ranging from 11 Å to 14 Å and applied axial pressures of 50 MPa to 500 MPa, they found that water can exhibit a first-order freezing transition to hexagonal and heptagonal ice nanotubes, and a

continuous phase transformation into solid-like square or pentagonal ice nanotubes. Concerning to answer the question what the unit cell of ice nanotube looks like for an *n*-gonal ice nanotube built from stacking a single type of *n*-gonal rings of water, the unit cell consists of two stacked *n*-gonal rings (Koga *et al.*, 2000a; Koga *et al.*, 2000b). The ring of O-H bonds of water molecules line up clockwise whereas in the other ring the O-H bonds line up as counterclockwise. Among the *n*-gonal ice nanotubes examined, the pentagonal or hexagonal ice nanotube appears to be the most stable. The phase diagram of water between hydrophobic surfaces (CNTs) was also studied by using *MD* simulations (Koga and Tanaka, 2005). There were two classes of quasi-two-dimensional solid water into which liquid water confined between hydrophobic surfaces freezes spontaneously and whose hydrogen-bond networks were as fully connected as those of bulk ice. It was found that the phase transformations among liquid, bilayer amorphous (or crystalline) ice, and monolayer ice phases at various thermodynamic conditions, then determined curves of melting, freezing, and solid-solid structural change on the isostress planes where temperature and intersurface distance were variable.

MD simulations have investigated the fundamental of diffusion mechanisms of water driving in nanoporous (Wang *et al.*, 2003). One talented area of studying nanotubes involved modeling them to mimic real ion channels in biological systems, which reduced the complexity of modeling ion channels. The properties of a nanotube strongly depend on its helicity; therefore the effect of helicity on behaviors of water molecules confined in nanotubes deserved further investigation. Behaviors of water molecules confined in (6,6) armchair and (10,0) zigzag types were analyzed by MD simulation at 300 K and 1.01×10^5 Pa. It was indicated that water molecules could flow into hydrophobic carbon tubes to form a stable hydrogen-bonded chain called single file, and spontaneously conduct through tubes as the single file form and the ability of water conduction through (10,0) zigzag tube was stronger than that through (6,6) armchair tube.

Many types of transportation in small pores, one type is called single-file transport of water molecules through a CNT (Berezhkovskii and Hummer, 2002). MD simulations of water transport through the interior channel of a carbon nanotube in contact with an aqueous reservoir showed that conduction occurred in bursts with collective water motion. A continuous-time random-walk model was used to describe concerted transport through channels densely filled with molecules in a single-file arrangement, found in zeolites, as well as in ion channels and aquaporins in biological membranes. Theoretical predictions for different collective properties of the single-file transport agree with the simulation results. Striolo reported the mechanism of water diffusion in narrow CNT. Results showed exceptional physical properties that render them promising candidates as building blocks for nanostructured materials (Striolo, 2006). Many ambitious applications, ranging from gene therapy to membrane separations, require the delivery of fluids, in particular aqueous solutions, through the interior of carbon nanotubes. To foster these and other applications, it was necessary to understand the thermodynamic and transport properties of water confined within long narrow carbon nanotubes. Previous theoretical study considered only either short carbon nanotubes or short periods of time. By conducting MD simulations in the microcanonical ensemble for water confined in infinitely long carbon nanotubes of diameter 10.8 Å (Striolo, 2006). It was found that confined water molecules diffuse through a fast ballistic motion mechanism for up to 500 ps at room temperature. By comparing the results obtained for the diffusion of water to those obtained for the diffusion of a reference LJ fluid, it proved that long-lasting hydrogen bonds was responsible for the ballistic diffusion of water clusters in narrow carbon nanotubes, as opposed to spatial mismatches between pore-fluid and fluid-fluid attractive interactions which, as shown previously by others (Liu *et al.*, 2005a; Striolo *et al.*, 2003; Striolo *et al.*, 2004a), were responsible for the concerted motion of simple fluids in molecular sieves. Additionally, Striolo proved for the first time that despite the narrow diameter of the CNTs considered which may suggested the existence of single-file diffusion, when the trajectories of confined water

were studied at time scales in excess of 500 ps, a Fickian-type diffusion mechanism prevails.

Dynamic Monte Carlo (MC) simulations and analytical calculations investigated the effect of pore surface roughness on Knudsen self- and Fickian diffusion in nanoporous media (Malek and Coppens, 2003). Principle of difference was found between the roughness dependence of the macroscopic, transport diffusivity and the microscopic, self-diffusivity, which was reminiscent of diffusion in zeolites, where a similar difference arises due to adsorption effects and intermolecular interactions. The differences become significant when the pore surface was rough down to molecular scales, as was the case, e.g., for many common sol-gel materials. The results showed that surface roughness could affect self-diffusivity of gas molecules in the Knudsen regime. On the other hand, the molecular trajectories in smooth and rough pores showed the independence of transport diffusivity on surface roughness. The projection of the molecular trajectory pathway in a pore with a rough surface was equivalent to that in a pore with a smooth surface when the molecule performs surface jumps around regions on the order of the diameter of the fjord inlet size. These jumps quickly decorrelate; therefore the transmission was roughness independent. These simulations were in good agreement with analytical calculations for several tested rough, fractal pore structures. The self-diffusivity was more fundamental diffusivity, expressing how the position of a molecule changes with the time as a result of its random motions, influenced by its environment. That environment influenced the total trajectory length. Their results were important for the interpretation of experimental diffusion measurements and for the study of diffusion-reaction processes in nanoporous catalysts with a rough internal surface.

Resemblance the MD simulations showed the Fickian water diffusion in (6,6)-armchair CNTs (Mukherjee *et al.*, 2007a). That size of the nanotube allowed only a single file of water molecules inside the nanotube. Water molecules inside that showed solidlike ordering at room temperature. It was shown that even for the longest

observation times, the mode of diffusion of the water molecules inside the nanotube was Fickian and not subdiffusive. It also proposed a one-dimensional random walk model for the diffusion of the water molecules inside the nanotube. That work calculated mean-square displacements (*MDS*) from the random walk model by MD simulations, thereby confirming that the water molecules underwent normal mode diffusion inside the nanotube. It was attributed this behavior to strong positional correlations that caused all the water molecules inside the nanotube to move collectively as a single object. There was good between the results from the model and MD simulation for the time scale (average residence time) of the exponential decay of the survival probability. This time scale was shown to depend on the length of the nanotube, which was another piece of evidence in support of the conclusion that the mode of diffusion was normal. Another case, water molecules inside narrow, open-ended carbon nanotubes placed in a bath of water molecules (Mukherjee *et al*., 2007b). The radius of the tube was such that only a single file of water molecules was allowed inside the tube. The calculated *MSD* of the confined water molecules reveals that initially the water molecules undergo ballistic motion that crosses over to normal (Fickian) diffusion at longer times.

Properties of boron nitride (BN) nanotubes have investigated (Ishigami *et al.*, 2003a; 2003b). Boron nitride nanotubes were expected to be as desirable for application as carbon nanotubes. Although boron nitride nanotubes were wide band gap semiconductors and electronics nearly insulating, scanning tunneling microscopy can be used to image and characterize them. The studied of electronic properties of BN nanotubes was used a low temperature scanning tunneling microscope (STM) operated at 7 K. STM images of the tubes reveal hexagonal lattices or stripe patterns, which can be caused by interlayer coupling or scattering of electronic states of the nanotubes. Scanning tunneling spectroscopies measurements indicate that the tubes have banded gaps exceeding 4 eV, and reveals van Hove singularities confirming the one-dimensional nature of electronic states of the nanotubes.

There are few theoretical studies of water confined in BNNT. Water permeation through in a subnanometer single-walled boron nitride nanotube (SWBNNT) reported by Won and Aluru (Won and Aluru, 2007). BNNTs possessed many excellent physical properties, including thermal and mechanical properties. They showed the superior water permeation properties of BNNTs by using MD simulation. Specifically, water molecule permeate through the (5,5)-SWBNNT nitride nanotube, while a (5,5)-SWCNT of approximate the same diameter did not conduct water. It suggested that the relatively strong interactions between the nitride atoms of the BNNT and water molecules play a key role in the continuous wetting behavior of the SWBNNT. The properties of water, such as the axial diffusion coefficient and the hydrogen bonding, inside the (5,5) SWBNNT were comparable to those inside the (6,6)-SWCNT, even though the diameter of the (5,5)-BNNT was 1.3 Å smaller than that of the (6,6)-SWCNT.

Other case, Won and Aluru studied water flow in (16,16)-SWCNTs and reported the flow rates from velocity jump in a depletion region at the water-nanotube interface and that the water orientations and hydrogen bonding at the interface significantly affected the water flow rates (Won and Aluru, 2008). It was found that nanotube with the same smooth wall structure but with more hydrophilic Lennard-Jones (LJ) parameters of silicon was deeply reduced because of there was not free OH bonds pointing to the wall as in CNTs that reduce the number of hydrogen bonds in the depletion layer. Another important point to note was that the flow rates were highly sensitive to the interatomic distances. The simulations of (16,16)-SWBNNT presented a B-N bond length of 0.144 nm, which is slightly more than 0.142 nm (the bond length for CNT). It was found that the water structure; OH bond orientations and the hydrogen bonding in the depletion region was less than 5% of the bulk value has a direct effect on the enhancement of flow rates. A unique combination of features such as hexagonal structure, interatomic distances and water orientations with free OH bonds pointing to the wall and the decreased hydrogen bonding in the depletion region contributed the large flow rates in SWCNTs.

There still have been lacks to studies on the water transmission properties of BNNTs. For more extremely study the fundamental insights into the water confined in SWBNNTs and to compare the results with those in CNTs. Therefore, the investigation on structural and dynamical of water confined in SWBNNTs is also of interest. The objectives of this work have focused into study the influence of attractive interactions between water and variance confining walls on structure and dynamics properties of water at density of 1.00 g cm^{-3}. MD simulations studied the effects of confined spaces on molecular distribution and transport behaviors of water confined in SWCNTs and SWBNNTs. Diffusion coefficients and molecular distribution functions of water confined in both nanotubes were discussed.

MATERIALS AND METHODS

Models and Simulation Details

The (*n*,*n*)-armchair type SWCNTs considered in this study were modeled as a rigid networks of uncharged Lennard-Jones (LJ) carbon atoms with C-C bond distances of 1.42 Å and a fixed nanotube length of 36.89 Å. To study the effects of nanotube diameter dependence on structure and dynamics properties of the confined water, the effective diameters of SWCNTs, after excluding the van der Waals radius of C atoms of 1.70 Å, were varied from 8.86 to 23.74 Å, corresponding to the armchair SWCNTs of n = 9, 10, 12, 14, 16 and 20, respectively. These nanotubes were filled with a total number of 77, 102, 162, 237, 327, and 547 water molecules, respectively, which led to an average water density of 1.00 g cm^{-3}. Details of the simulation runs are showed in Table 1.

Table 1 Details for the MD simulation runs of water in carbon- and boron-nitride nanotubes in this work. The length is 36.89Å in all cases.

Nanotubes model	Real / Van der Waals diameter (Å)	Number of water (molecules)	Periodic box size X × Y × Z ($Å^3$)	Simulation run (ns)
Bulk water	-	1,000	31.03 × 31.03 × 31.03	1
(9,9)-SWCNT, -SWBNNT	12.26 / 8.86	77	24.52 × 24.52 × 36.89	4
(10,10)-SWCNT, -SWBNNT	13.62 / 10.22	102	27.24 × 27.24 × 36.89	4
(12,12)-SWCNT, -SWBNNT	16.32 / 12.92	162	32.64 × 32.64 × 36.89	1
(14,14)-SWCNT, -SWBNNT	19.02 / 15.62	237	38.04 × 38.04 × 36.89	1
(16,16)-SWCNT, -SWBNNT	21.74 / 18.34	327	43.48 × 43.48 × 36.89	1
(20,20)-SWCNT, -SWBNNT	27.14 / 23.74	547	54.28 × 54.28× 36.89	1

Water was described by the extended simple point charge (SPC/E) model ($\varepsilon_{O\text{-}O}$ = 0.1554 kcal mol^{-1} and $\sigma_{O\text{-}O}$ = 3.16 Å) (Berendsen *et al.*, 1987; Guillot, 2002). The geometry of each water molecule was held rigid using the SHAKE algorithm. Two hydrogen atoms were located from the oxygen center by 1.0 Å with an H-O-H angle of 109.5°. Atomic charges of −0.8476*e* and +0.4238*e* were assigned to oxygen and hydrogen sites, respectively (see Figure 4).

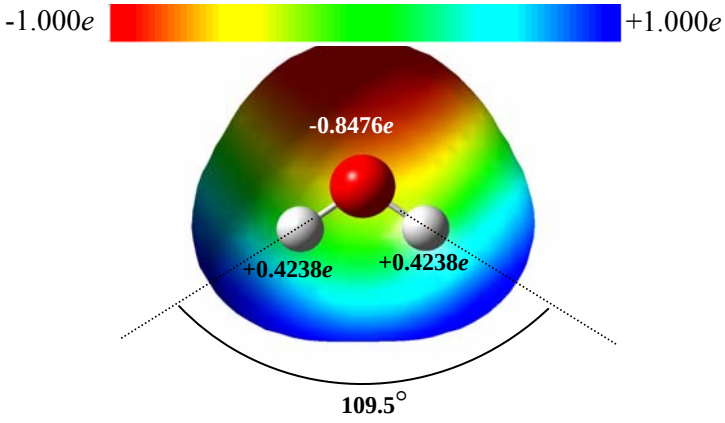

Figure 4 Positive and negative charges surface area described the extended simple point charge (SPC/E) of water model. Isovalue for surface is 0.0004.

Interactions between water and the nanotube wall were described by the 12-6 LJ potential. The LJ parameters for carbon ($\varepsilon_{C\text{-}C}$ = 0.0970 kcal mol^{-1} and $\sigma_{C\text{-}C}$ = 3.36 Å) were taken from Mashl *et al.*, 2003:

$$U(r_{ij}) = 4\varepsilon_{ij}\left[\left(\frac{\sigma_{ij}}{r_{ij}}\right)^{12} - \left(\frac{\sigma_{ij}}{r_{ij}}\right)^{6}\right] \qquad (2)$$

where ε_{ij} and σ_{ij} symbolize the size and strength of the LJ potential parameters, and r_{ij} is the distance between the centers of mass of the pair atoms. The water-nanotube interaction parameters were derived by using the Lorentz-Berthelot combining rules i.e. $\varepsilon_{ij} = (\varepsilon_i \varepsilon_j)^{1/2}$ and $\sigma_{ij} = (\sigma_i + \sigma_j)/2$, where ε_{ij} and σ_{ij} are of the LJ potential parameters between sites *i* and *j*. Lennard-Jones potential parameters are listed in Table 2.

Table 2 The Lennard-Jones (LJ) potential parameters for pair atoms interactions use in this work.

Atom-atom Interactions	σ_{ij} (Å)	ε_{ij} (kcal mol^{-1})
O_{water}-O_{water}	3.166	0.1554
C_{CNT}-O_{water} (a)	3.260	0.1144
C_{CNT}-O_{water} (b)	3.260*	0.1230*
B_{BNNT}-O_{water}	3.260	0.1215
N_{BNNT}-O_{water}	3.260	0.1501

Source: * Mashl *et al.* (2003)

The degree of "nanotube hydrophobicity" was varied for all tubes by changing the strength of LJ potential parameter (ε_{O-C}) between water and the nanotube wall as an independent parameter, keeping the size parameter (σ_{C-C}) unchanged. The hydrophobicity was increased by reducing the ε_{O-C} = 0.1143 kcal mol^{-1} (7% reduction) compared to the full value ε_{O-C} = 0.1230 kcal mol^{-1}. These simulations were labeled a, e.g. (9,9)-SWCNTa; simulations with the full potential were labeled to b. Furthermore, this work studied a case which models boron nitride nanotubes (SWBNNT) isostructural to the carbon nanotubes. Still keeping the σ-value constant, we set ε = 0.1216 kcal mol^{-1} and 0.1502 kcal mol^{-1} for the oxygen-boron and oxygen-nitrogen interactions, respectively, as in the work of Won and Aluru, 2000. Already the 7% decrease in hydrophobicity was found to lead to a loss of water conductivity in the (5,5)-SWCNT (Won and Aluru, 2007). Similarly, it was found that in (5,5)-armchair single-walled boron nitride nanotubes (SWBNNT) attractive interactions between water and nitrogen sites were primarily accountable for the good water conduction ability. Therefore, it seemed interesting to look at the diffusion and structural properties of water confined in large diameter tubes also of this type. A pure water box at 298 K was also run for comparison.

The coordinates for the wall atoms were generated with the "Materials Studio" version 4.1 licensed from NANOTEC Thailand. Short pieces of tube were then surrounded by about 2000 SPC/E water molecules in simulation box and *NPT* simulations were started with P = 1 atm and temperature lowered from high values to T = 298 K. In a few 10 picoseconds, depending on tube size, the small sections of the tubes were filled with water. Several of these pieces, details see below, were then put together in periodic box and equilibrated before starting the production runs.

All MD simulations were performed in the canonical (*NVT*) ensemble at a temperature of 298 K by using the Nosé-Hoover thermostat implemented in the DL_POLY program package, version 2.17 (Smith *et al.*, 2006). The dimensions of the periodic simulation box for each system were twice the nanotube diameter in the *x*- and *y*- directions and the length of natube in the *z*-direction. The principle axis of the nanotubes was superimposed onto the *z* axis of the simulation box. Periodic boundary conditions were applied to all three directions. The long-range electrostatic interactions between water molecules confined in SWCNTs were computed by using the Ewald method and the short-range van der Waals interactions are computed using the cutoff radius equal to the nanotube diameter (for n = 9, 10, and 12) and 18.44 Å (for n = 14, 16, and 20). The equations of motion were integrated with a 0.25-fs time step to ensure that there was no drift of energy and temperature throughout the simulations. Starting geometry of the simulation runs are presented in Figure 5.

The systems were equilibrated to the required temperature for 0.25 ns using the velocity rescaling algorithm. After equilibration period, the velocity rescaling was removed and the production runs were conducted for up to 1 ns. During the production runs, the coordinates and velocities were stored every 50 fs for further analyses.

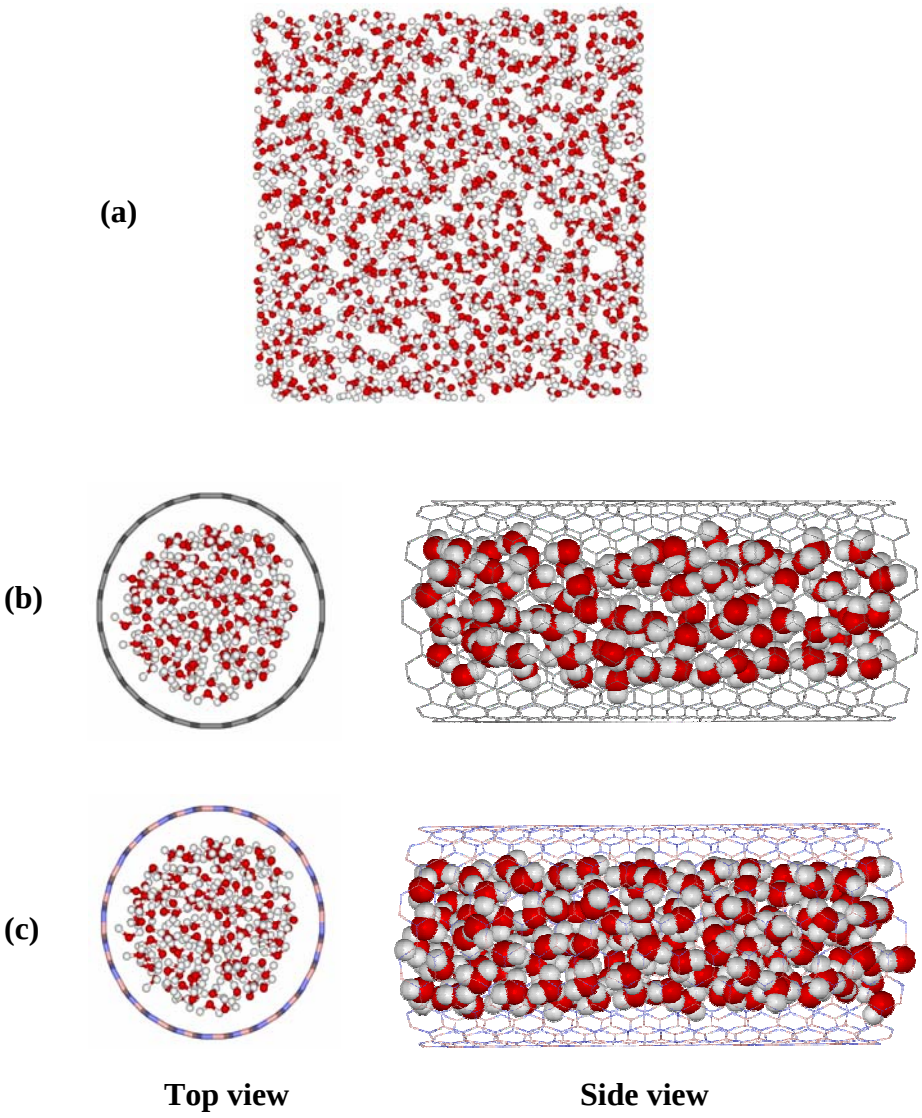

Figure 5 Starting geometry of bulk water**(a)**, water 162 molecules in (12,12)-SWCNT**(b)** and water 162 water molecules in (12,12)-SWBNNT**(c).**

The structure was analyzed by using the pair radial distribution function (*RDF*), $g_{AB}(r)$, specified by the average position r from the center of atom A and B (O_{water} - O_{water}), and r was the radial distance measured in concentric spherical shells from the center of atom A (O_{water}) and cylindrical $g(r)$ distribution functions of water with respect to the center of nanotubes which defined as

$$g_{AB}(r) = \left\langle \frac{dn_{AB}}{dr} \frac{1}{4\pi r^2 \rho_B N_A} \right\rangle \tag{3}$$

where N_A is the number of A centers, ρ_B is the macroscopic density of the B centers and n_{AB} is the number of AB pairs.

The molecular diffusion was analyzed by molecule travels through the time movement of the mean square displacement (*MSD*), which is Einstein expression defined as

$$MSD(t) = \left\langle \left| r_i(t) - r_i(t_0) \right|^2 \right\rangle \tag{4}$$

MSD of confined water molecules was computed in the (*x, y, and z*) directions. The slope of the *MSD* (t) was considered for sufficiently long time for it to be in the linear rule, was related to the self-diffusion constant D:

$$D = \frac{1}{\delta} \lim_{t \to \infty} \frac{d\left\langle \left| r_i(t) - r_i(t_0) \right|^2 \right\rangle}{dt} \tag{5}$$

where δ depends on the space dimensionality; 6 for three dimensions, 4 for two dimensions and 2 for a dimension.

RESULTS AND DISCUSSION

In early work, the simulation runs used a time step of 1.00 fs, and it was found that the system was not going to balance condition. The total energies of bulk water and water confined in nanotubes rose up at the long simulation time (see in Figure 6-left). Although the total energy was not equilibrated, the temperature was well averaged at 298 K. The increase of total energy suggests that the systems were not stable. Therefore, a small time step of 0.25 fs was used and found to be good for the simulation in the canonical *NVT* ensemble with Nosé-Hoover thermostat. Equilibration ensemble was confirmed by the constant of total energy diagram (Figure 6, right hand side). Total energy of bulk water fluctuated within 1.0 kcal mol^{-1} (Figure 6 (a), right), water 77 molecules in (9,9)-SWBNNT fluctuated within 0.08 kcal mol^{-1} (Figure 6 (b), right), water 102 in (10,10)-SWBNNT fluctuated within 0.2 kcal mol^{-1} (Figure 6 (c), right) and other systems see at the second column in Table 3.

Additionally, the total angular momentum was also checked. The total angular momentum of *x*, *y* and *z* components of bulk water (1,000 molecules) were steady at zero (see Figure 7). The total angular momentum of water confined in nanotubes, the smallest tube (water 77 molecules in (9,9)-armchair nanotubes as shows in Figure 8), and the angular momentum *x*, *y* and *z* components were diverting from zero, as it is known that when using periodic boundary conditions, the angular momentum is not conserved.

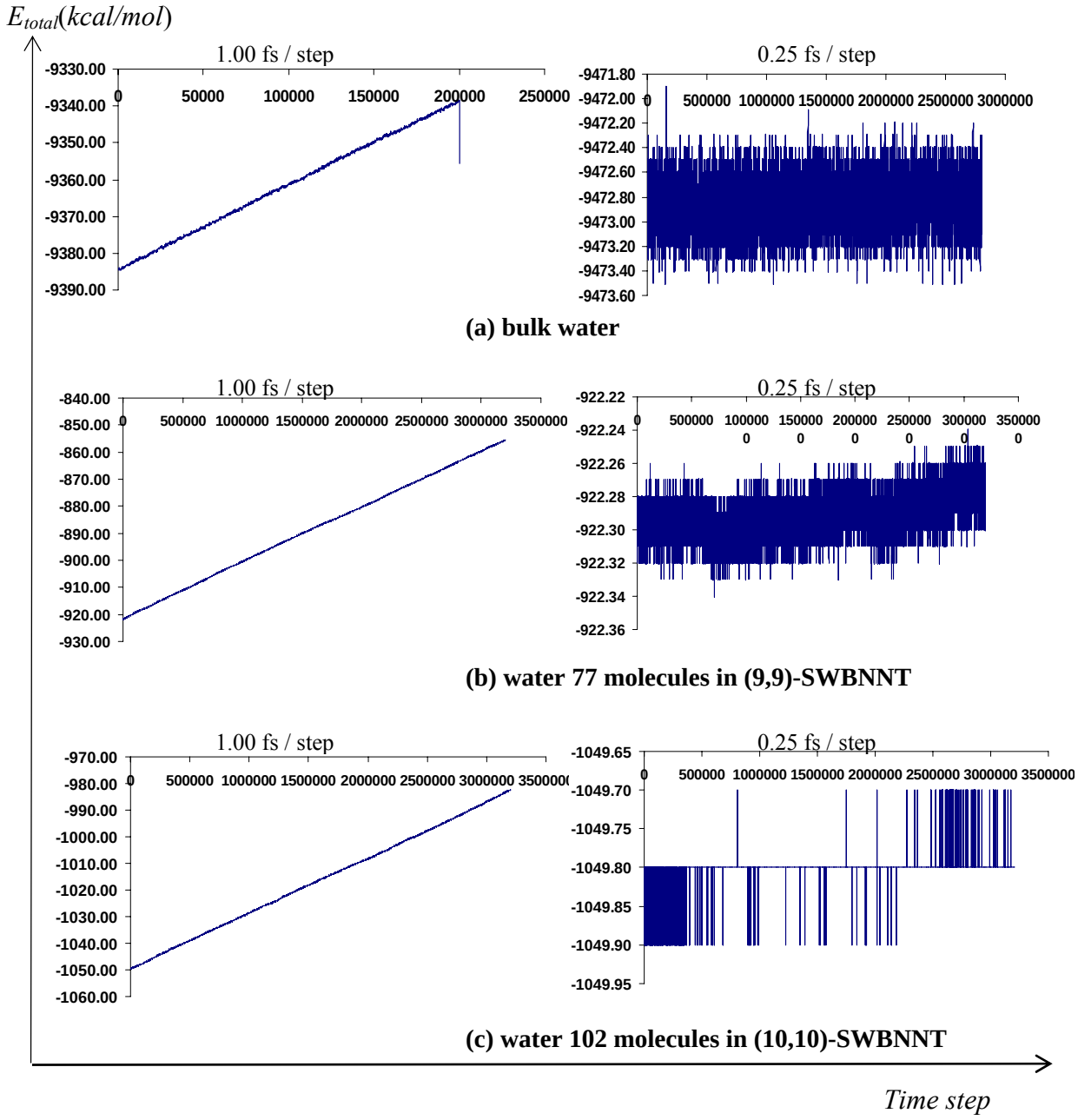

Figure 6 Total energy (kcal mol^{-1}) diagrams show the equilibration of the *NVT* ensemble with Nosé-Hoover thermostat at value of 1.00 fs per a time step (left) and 0.25 fs per a time step (right): total energy of bulk water **(a)**, water 77 molecules in (9,9)-SWBNNT **(b)** and water 102 molecules in (10,10)-SWBNNT **(c).**

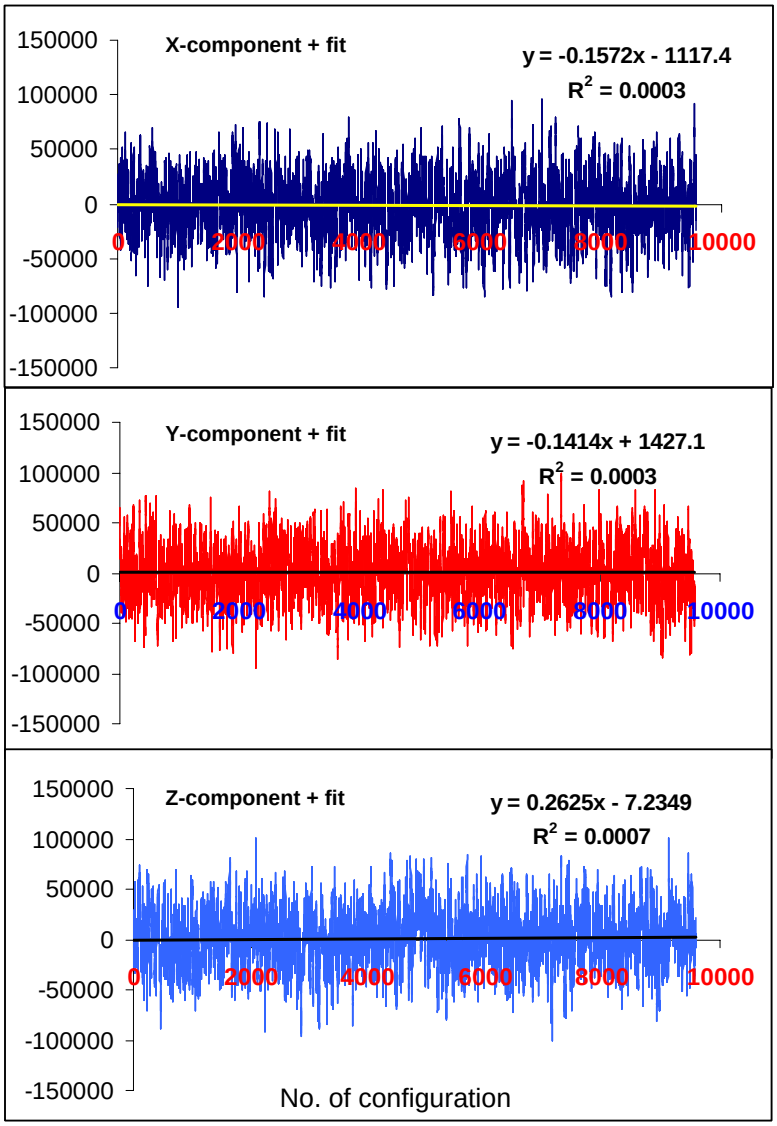

Figure 7 Angular momentum diagram of systems show equilibration state of the *NVT* ensemble with Nosé-Hoover thermostat at value of 0.25 fs per a time step of bulk water (water 1,000 molecules).

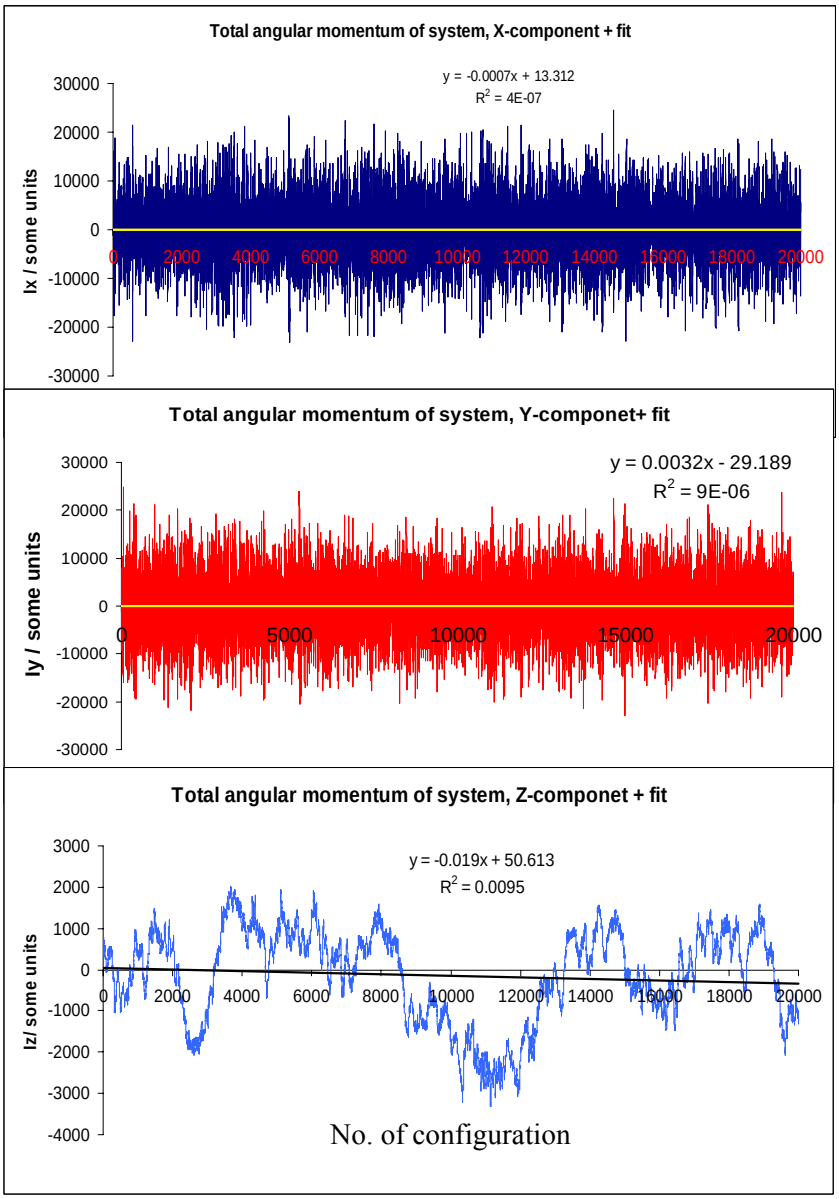

Figure 8 Angular momentum diagrams show equilibration state of the *NVT* ensemble with Nosé-Hoover thermostat at value of 0.25 fs per a time step of water 77 molecules (9,9)-SWBNNTs.

Table 3 Average of total energy (kcal mol^{-1}) and angular momentum (rad s^{-1}) of equilibration systems.

Model	**Average of total energy (kcal mol^{-1})**			**Average of angular momentum of system: Ix, Iy, Iz component**
Bulk water				3×10^{-4}, 3×10^{-4}, 7×10^{-4}
ε_{co} = 0.11433 kcal/mol				
(9,9) - SWCNTa	-885.480	±	0.012	3×10^{-6}, 2×10^{-7}, 8×10^{-2}
(10,10) - SWCNTa	-1041.802	±	0.015	9×10^{-6}, 1×10^{-5}, 3×10^{-4}
(12,12) - SWCNTa	-1591.707	±	0.029	1×10^{-5}, 6×10^{-6}, 3×10^{-2}
(14,14) - SWCNTa	-2302.486	±	0.043	1×10^{-5}, 3×10^{-5}, 3×10^{-3}
(16,16) - SWCNTa	-3156.582	±	0.060	7×10^{-6}, 1×10^{-5}, 1×10^{-3}
(20,20) - SWCNTa	-5373.613	±	0.094	2×10^{-4}, 2×10^{-4}, 4×10^{-4}
ε_{co} = 0.12300 kcal/mol				
(9,9) - SWCNTb	-904.770	±	0.010	6×10^{-8}, 1×10^{-5}, 2×10^{-2}
(10,10) - SWCNTb	-1068.551	±	0.050	2×10^{-5}, 2×10^{-6}, 1×10^{-2}
(12,12) - SWCNTb	-1621.994	±	0.026	2×10^{-7}, 4×10^{-6}, 7×10^{-3}
(14,14) - SWCNTb	-2360.827	±	0.048	9×10^{-5}, 5×10^{-6}, 6×10^{-3}
(16,16) - SWCNTb	-3217.884	±	0.057	3×10^{-6}, 8×10^{-5}, 1×10^{-3}
(20,20) - SWCNTb	-5376.137	±	0.092	3×10^{-4}, 4×10^{-4}, 4×10^{-3}
(9,9) - SWBNNT	-922.298	±	0.010	4×10^{-7}, 9×10^{-6}, 9×10^{-3}
(10,10) - SWBNNT	-1049.805	±	0.021	4×10^{-5}, 1×10^{-6}, 3×10^{-3}
(12,12) - SWBNNT	-1653.444	±	0.050	4×10^{-4}, 2×10^{-5}, 2×10^{-2}
(14,14) - SWBNNT	2431.186	±	0.046	7×10^{-5}, 2×10^{-6}, 2×10^{-2}
(16,16) - SWBNNT	-3287.572	±	0.059	1×10^{-5}, 8×10^{-6}, 1×10^{-3}
(20,20) - SWBNNT	-5373.618	±	0.094	1×10^{-4}, 3×10^{-4}, 7×10^{-4}

Structure comparison of bulk water molecules and water molecules enclosed in different sizes of nanotubes

The radial distribution function (RDF) of water was extracted from the simulation after the system was in equilibrium, and was interpreted to understand the molecular distribution and structure properties of water systems at the deeply molecular level. The results of the radial distribution profiles of bulk water were closed to the results of the neutron diffraction experiment (Soper, 2000). Figure 9 shows the average maximum distances following the 1^{st}, 2^{nd}, 3^{rd} hydration shells: OO distribution of 2.75, 4.55 and 6.79 Å, OH of 1.0, 1.77 and 3.25 Å, and HH of 1.63, 2.40 and 3.99 Å, respectively. The experimental data from neutron diffraction (Kuhs *et al.*, 1984) at 10 K 2.4 GPa reported that the R_{OO} distances were 2.879 and 2.742 Å for H-bonded and non- H-bonded, respectively.

The comparative RDF of bulk water and water confined in nanotubes are shown in Figure 10. The first maximum of all radial distribution functions occurs as a sharp peak at 2.75 - 2.76 Å. The details of the first maximum, first minimum and the average of coordination number n (r) of confined water are presented in the Table 4.

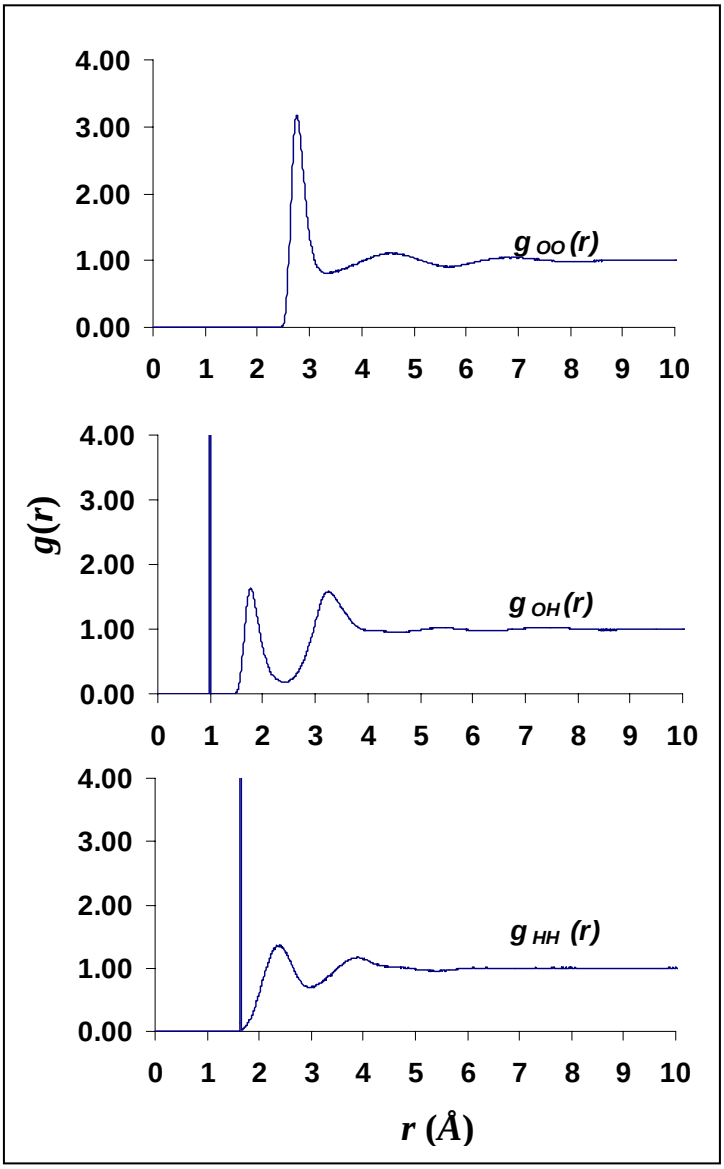

Figure 9 The spherical radial distribution function (RDF) of bulk SPC/E water (1,000 molecules); the partial structure factors of $g_{OO}(r)$, $g_{OH}(r)$ and $g_{HH}(r)$ at the average temperature of 298 K and the water density of 1.00 g cm^{-3}.

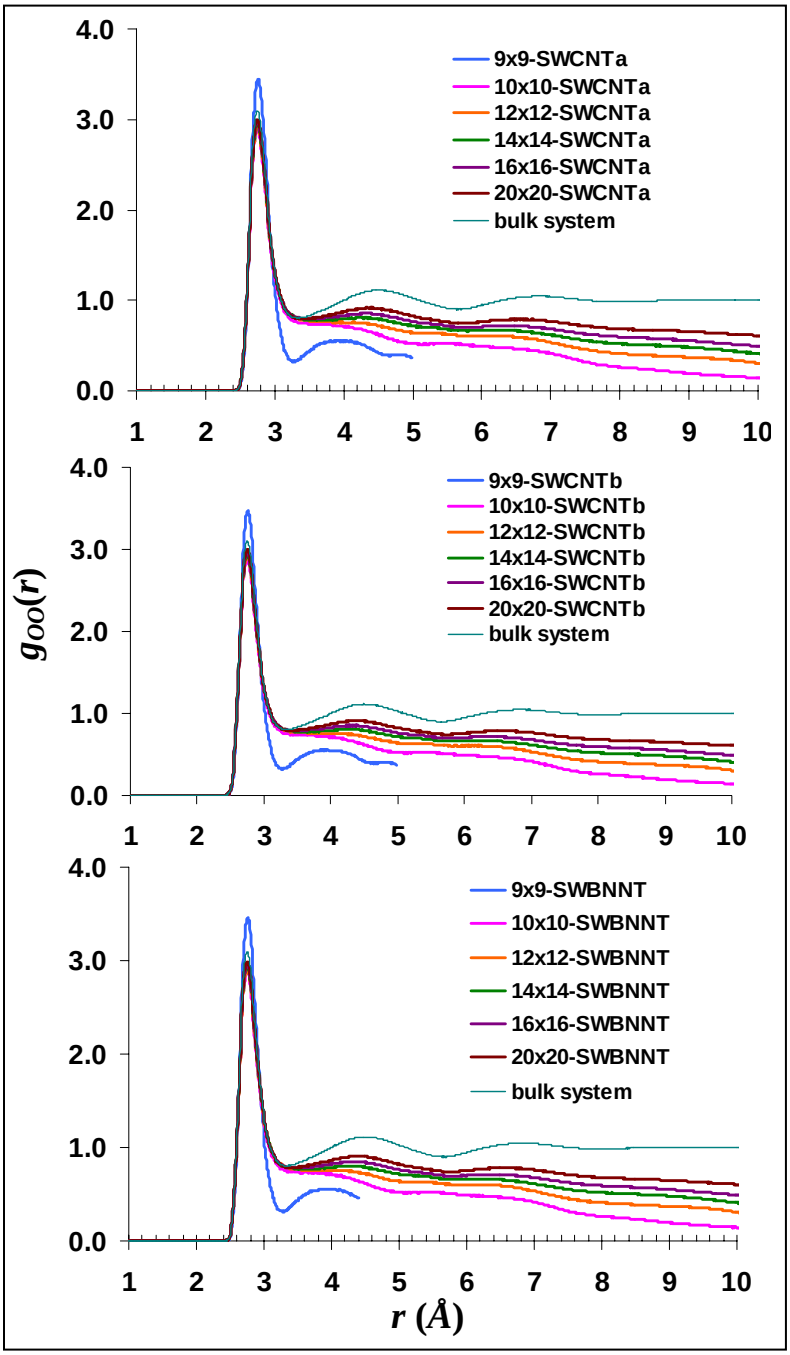

Figure 10 The spherical radial distribution function (RDF) $g_{OO}(r)$ of water confined in SWCNTa of $\varepsilon_{c\text{-}o}$ = 0.1143 kcal mol^{-1} **(a)**, SWCNTb $\varepsilon_{c\text{-}o}$ = 0.1230 kcal mol^{-1} **(b)** and SWBNNT **(c)**; (9,9)-nanotubes: blue, (10,10)-nanotubes: pink, (12,12)-nanotubes: orange, (14,14)-nanotubes: green, (16,16)-nanotubes: violet, (20,20)-nanotubes: brown and bulk system: soft green at the average temperature of 298 K and the water density of 1.00 g cm^{-3}.

Table 4 The results of first maximum and first minimum positions of spherical radial distribution profile $g_{OO}(r)$ of water confined in nanotubes and the average coordination numbers $n(r)$.

Model	**1st Maximum** $g_{OO}(r)$ **(Å)**	**1st Minimum** $g_{OO}(r)$ **(Å)**	**1st Minimum** ***n*(*r*)**
Bulk water	2.75	3.33	4.50
$\varepsilon_{co} = 0.11433$ kcal mol^{-1}			
(9,9) - SWCNTa	2.75	3.27	4.00
(10,10) - SWCNTa	2.75	3.49	4.84
(12,12) - SWCNTa	2.75	3.42	4.71
(14,14) - SWCNTa	2.75	3.46	4.86
(16,16) - SWCNTa	2.75	3.42	4.73
(20,20) - SWCNTa	2.75	3.42	4.70
$\varepsilon_{co} = 0.12300$ kcal mol^{-1}			
(9,9) - SWCNTb	2.76	3.29	4.00
(10,10) - SWCNTb	2.75	3.48	4.79
(12,12) - SWCNTb	2.75	3.49	4.93
(14,14) - SWCNTb	2.75	3.46	4.85
(16,16) - SWCNTb	2.75	3.42	4.72
(20,20) - SWCNTb	2.75	3.42	4.65
(9,9) - SWBNNT	2.76	3.29	3.99
(10,10) - SWBNNT	2.75	3.48	4.79
(12,12) - SWBNNT	2.75	3.48	4.88
(14,14) - SWBNNT	2.75	3.46	4.83
(16,16) - SWBNNT	2.75	3.46	4.82
(20,20) - SWBNNT	2.75	3.44	4.79

In principle, liquid water is classified as a tetrahedral liquid, its coordination number defined as the area under the first peak of the oxygen-oxygen radial distribution function, $g_{OO}(r)$. Based on a geometric definition of averaging over all OO pairs closer than the first minimum in $g_{OO}(r)$, an $n(r)$ above four and below five suggests the presence of liquid water and the four directional hydrogen bonds of ice-like tetrahedral structure (Head-Gordon and Johnson, 2006). According the principle, it was found that the coordination number $n(r)$ of water confined in nanotubes which different attractive interactions of SWCNTa, SWCNTb and SWBNNT are not homogeneous. It is modified by confinement in the nanometer scale regions inside nanotubes. The water confined in smallest (9,9)-SWCNTa, (9,9)-SWCNTb and (9,9)-SWBNNT had an average $n(r)$ at four, and which indicated the ice-like property. While, water in the larger pore diameters (10,10), (12,12), (14,14) (effective diameters of 10.22, 12.92 and 15.62 Å respectively), $n(r)$ is increased. The $n(r)$ is slightly decreased on the effective diameters of 15.62, 18.34 and 23.74 Å: (14,14), (16, 16) and (20,20) respectively. All $n(r)$ of water in the wider pore sizes suggested the liquid-like properties.

The coordination number $n(r)$ and distribution percentage of coordination number were reported because there may be several distribution structures. In case of bulk water, there are coordination numbers of about 4 and 5 as shown in Figure 11. The average $n(r)$ is 4.50. It means that bulk water was in a form of liquid water. A snapshot of tetrahedral structure shows water 4 and 5 molecules surrounding water in the center see in Figure 11c. When water molecules are confined in nanotubes, their configurations differ from those in the bulk phase. Water molecules try to position themselves into shells inside the pores. For the (9,9) nanotube, all the water molecules are located close to the wall of the nanotube and the highest distribution of the coordination number is 4. The reason for the coordination of water molecules in the (9,9) nanotube being less than that in bulk water is the interactions between water molecules and the nanotube wall. These strong interactions combine with very limited space result in decreasing the number of water molecules that interact with one another. It seems that water behaves as the ice-like

structure. A cross section of a snapshot illustrates that water formed the single hexagonal ring inside (9,9)-nanotubes (see Figure 12a (*right*)).

In larger nanotubes, (10,10) SWCNTa, -SWCNTb and –SWBNNT, the major $n(r)$ distribution are 5 and 4 with the average $n(r)$ of 4.84 (SWCNTa), 4.79 (SWCNTb) and 4.79 (SWBNNT). Most of the water molecules in the middle of the pore are supposed to have a coordination number equal to 5, while the water molecules that locate close to the pore wall have a coordination number equal to 4. The trend of the ratio between the coordination numbers 4 and 5 is found to increase with increasing the nanotube size (see Figure 12(b-f)). This means that when the size of the nanotube increases, the water molecules will behave in the same way as in the bulk phase. However, the ratio between the coordination numbers 4 and 5 in the (10,10) nanotube is quite high. This probably results from the large amount of water molecules close to the wall. A cross section snapshot shows a single ring and near the tube wall and a water column at the center of nanotube. Its coordination number was in the range of liquid. This result indicating that the water confined in (10,10)-nanotubes have structural properties in between ice and liquid water properties. For the wider diameters, (12,12), (14,14), (16,16) and (20,20)-SWCNTa,-SWCNTb and –SWBNNT, the maximum $n(r)$ distribution is 5, following with 4, 6, 3, 8. The average $n(r)$ distribution indicated the liquid water structure.

Although the $n(r)$ distributions of water inside (10,10), (12,12), (14,14), (16,16) and (20,20) nanotubes were similar, the different arrangements were observed (inset snapshots in Figure 12 (*right*)). In the largest nanotube (20,20), confirmed water appeared to be bulk water character. In smaller tubes, (12,12) and (14,14) multi-layer of concentric rings can be observed from snapshots in Figure 12.

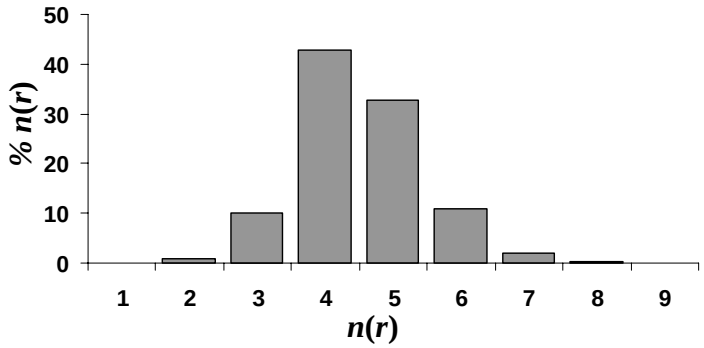

(a) Histogram of percentage $n(r)$ distribution of bulk water

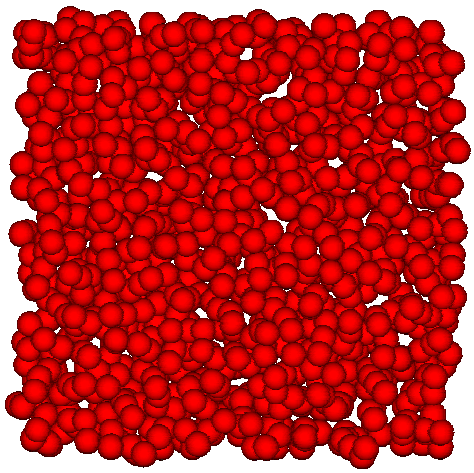

(b) A snapshot of bulk water

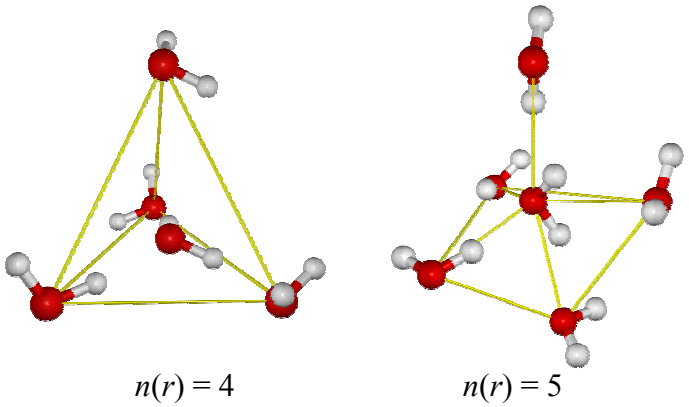

(c) Snapshot of tetrahedral structures

Figure 11 Structure of coordination number distribution of bulk water

a) Histogram of percentage $n(r)$ distribution of bulk water

b) A snapshot of bulk water

c) Snapshot of tetrahedral structures

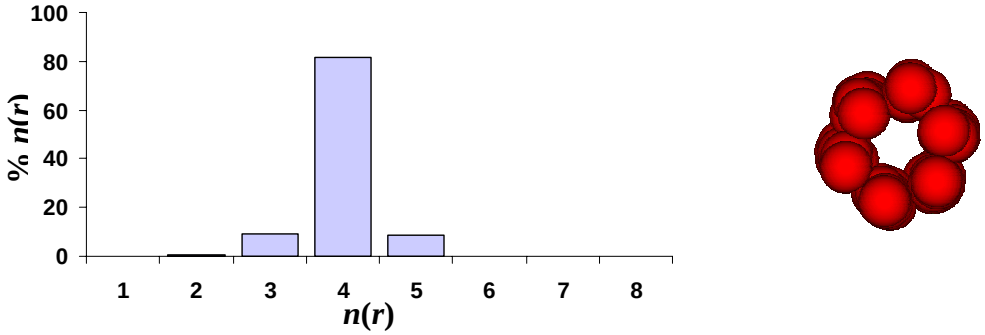

(a) water 77 molecules in (9,9)-SWBNNT

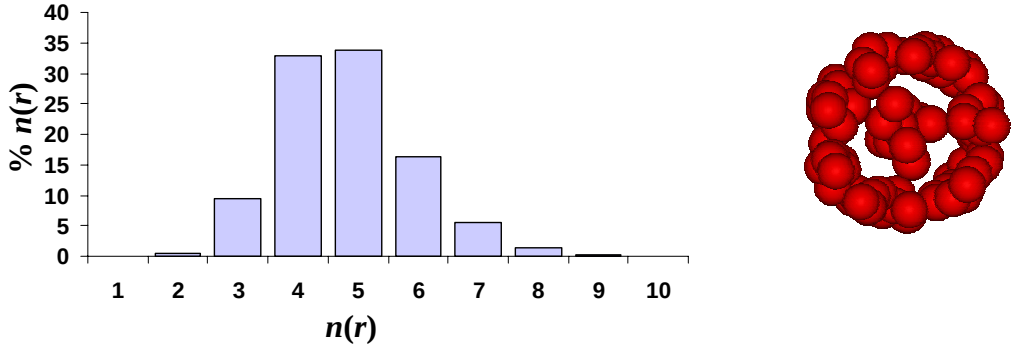

(b) water 102 molecules in (10,10)-SWBNNT

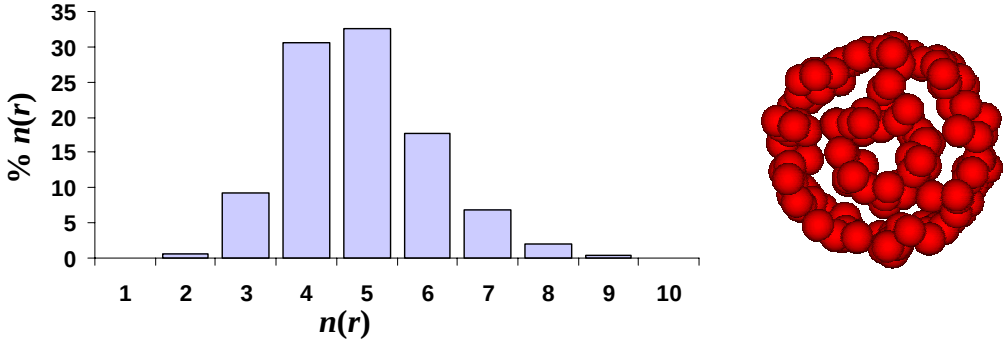

(c) water 162 molecules in (12,12)-SWBNNT

Figure 12 Histogram of coordination number distribution of water in SWBNNT (*left*) and inset cross section snapshots (*right*).

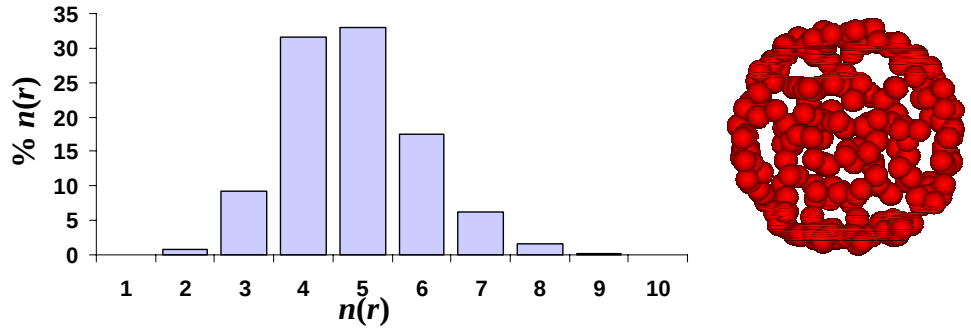

(d) water 237 molecules in (14,14)-SWBNNT

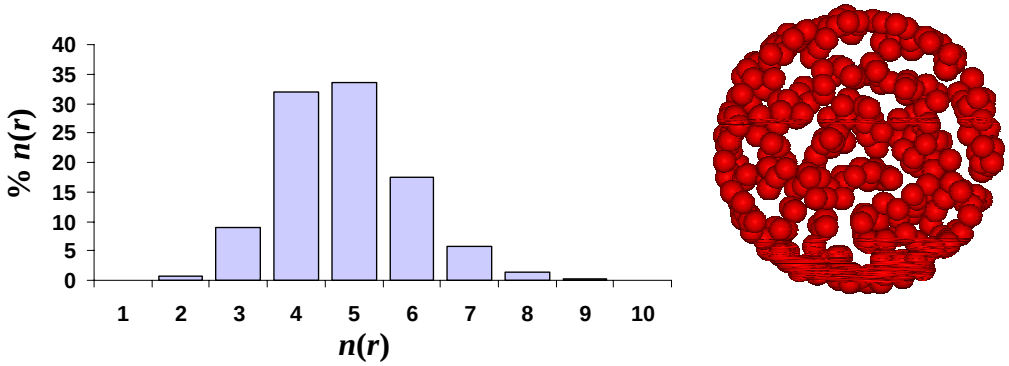

(e) water 327 molecules in (16,16)-SWBNNT

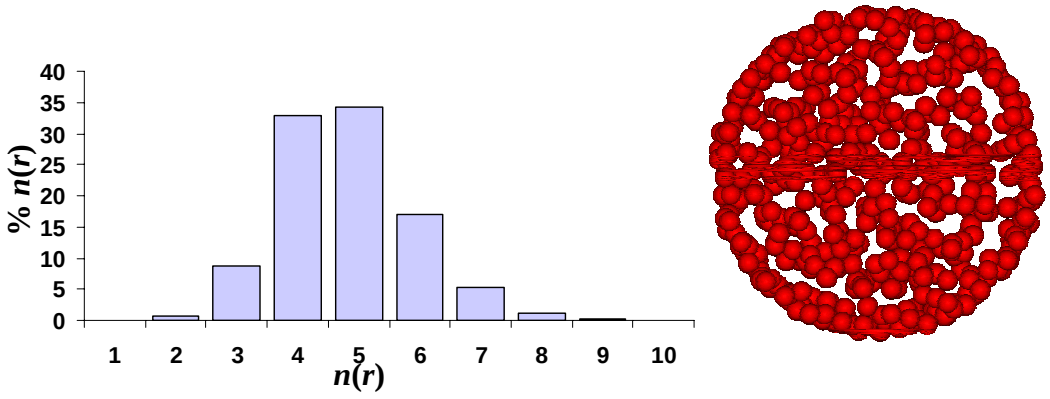

(f) water 547 molecules in (20,20)-SWBNNT

Figure 12 Histogram of coordination number distribution of water in SWBNNT (*left*) and inset cross section snapshots (*right*). (Cont'd)

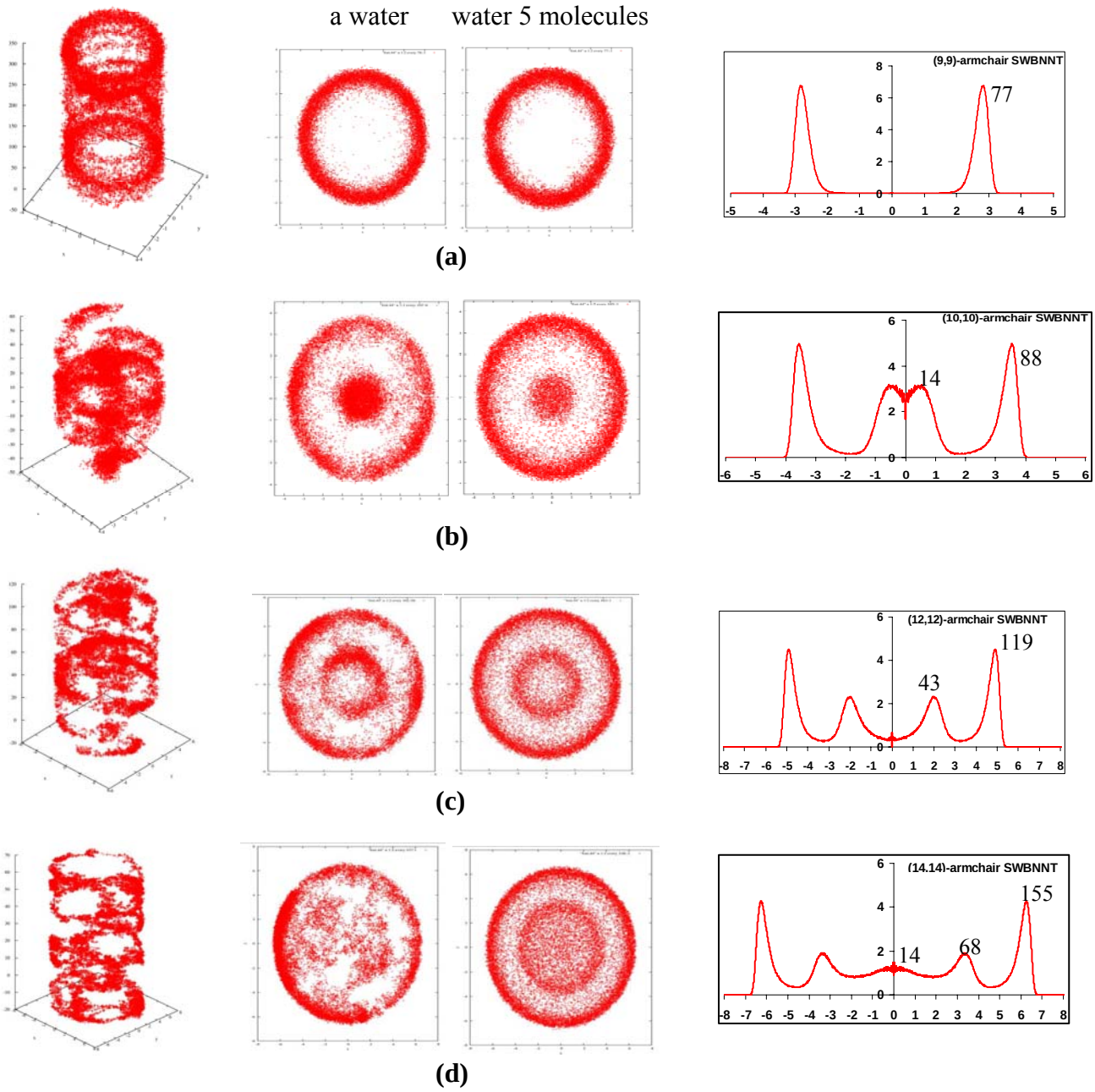

Figure 13 Three-dimensional distribution trajectories (*left*) of a selected water molecule in (9,9)- **(a)**, (10,10)- **(b)**, (12,12)- **(c)**, (14,14)- **(d)**, (16,16)- **(e)** and (20,20)- **(f)** armchair SWBNNTs; their projections onto the *xy* plane (*middle*); and cylindrical $g(r)$ distribution functions of water with respect to the center of those SWBNNTs (*right*).

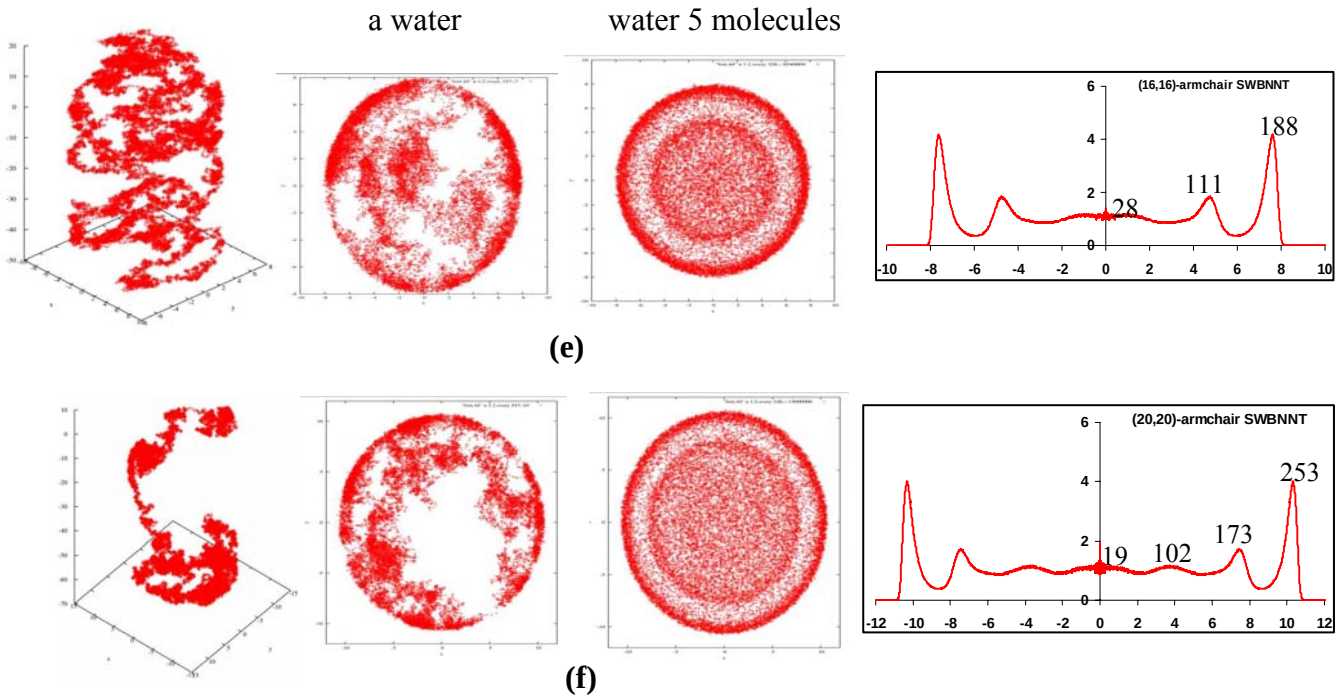

Figure 13 Three-dimensional distribution trajectories (*left*) of a selected water molecule in (9,9)- **(a)**, (10,10)- **(b)**, (12,12)- **(c)**, (14,14)- **(d)**, (16,16)- **(e)** and (20,20)- **(f)** armchair SWBNNTs; their projections onto the *xy* plane (*middle*); and cylindrical $g(r)$ distribution functions of water with respect to the center of those SWBNNTs (*right*). (cont'd)

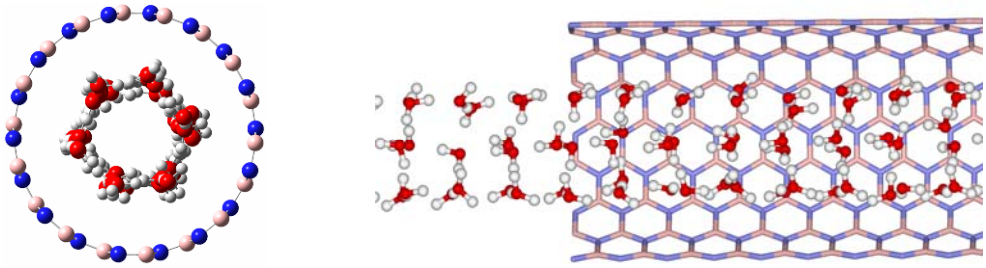

(a) **(b)**

Figure 14 Top view **(a)** and side view **(b)** of a snapshot of the six-membered ring structure of the single-walled ice-like nanotube in a (9,9)-armchair SWBNNTs.

Figures 13(a-f) show on right hand side, the cylindrical $g(r)$-functions across the boron-nitride nanotubes. The numbers above the curves refer to the average number of water molecules present in the various regions; the total number of molecules is listed in Table 1. The left hand side of the figures gives a visual impression by showing, at regular time intervals, x and y-coordinates of a one (*left*) and five (*right*) water molecules during the simulations. It shows that, except in the narrowest tube ((9,9)-nanotubes), where there is not enough space, molecules exchange frequently between the boundary layer and the inside of the tube.

The functions for the other two cases, SWCNTa and SWCNTb, are very similar to Figure 13(a-f) and are therefore not shown here. The boundary-layer peaks are slightly enhanced with increasing wall-water interactions, as expected. As an example, this work find an average of 250, 252, and 254 water molecules in the boundary layer in the cases SWCNTa, SWCNTb, and SWBNNT, respectively.

The cylindrical RDF of water molecules inside the nanotube obviously shows shell like configurations. In the (9,9) nanotube, most water molecules locate close to the wall and there is no water molecule located in the middle of the pore. This results from the attractive interactions between water molecules and the pore wall.

For the wider nanotube pore sizes, some water molecules still locate close to the pore wall and the excess water molecules form a ring like structure in the middle of pores. In the (10, 10) nanotube, the cylindrical RDF shows two maximum peaks. The distance between the two maximum peaks is 3.00 Å, which is significantly higher than that in the (12,12), (14,14), (16,16) and (20,20): (2.89, 2.89, 2.91 and 2.92 Å, respectively). These may result from the attraction between the water molecules in the middle of the pore in the (10,10) nanotube. Moreover, it was also found that there is less water exchange between the layers in the (10,10) nanotube and the exchange increases when the pore sizes increase.

Figures 13e and 13f show that above a diameter of about 18 Å the water density at the center is close to bulk density, about 1 g cm^{-3}. In narrower tubes, Figures 13b, 13c and 13d, the wall-induced layering leads to oscillations of the water density extending to the center. In the narrowest tube, Figure 13a, there is space for just one layer of water next to the wall, and the density at the center is negligible, in keeping with the results by Mashl et al. (Mashl *et al.*, 2003) for their (9,9) single wall nanotube.

Furthermore, the strong attractive interactions induced water molecules form the ice-like single-shell hexagonal structure inside the (9,9)-nanotubes (SWCNTa, SWCNTb and SWBNNT) as showed in Figure 14, it is similar to previous work (Marshl *et al.*, 2003).

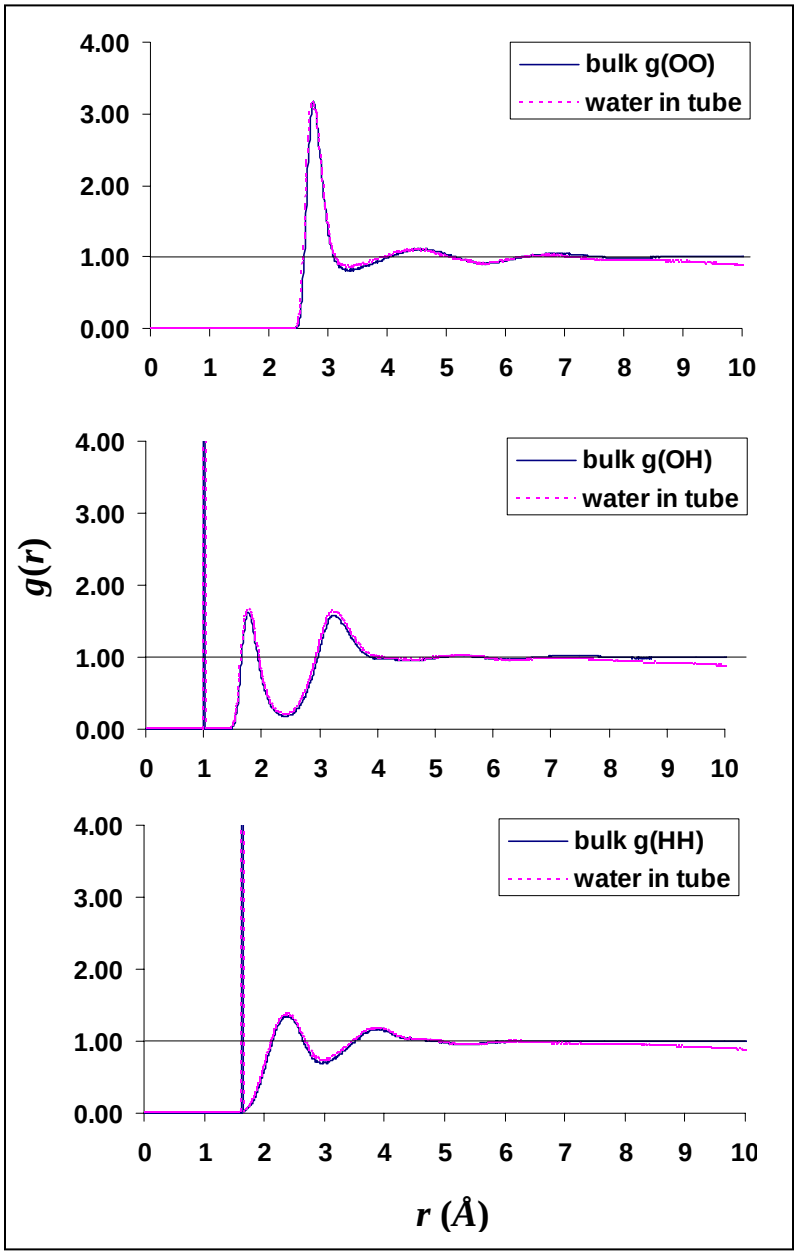

Figure 15 Radial distribution functions g_{OO}, g_{OH}, and g_{HH} for pure water (solid) and for water molecules in the center (-2.2 Å < r < 2.2 Å) of the (20,20) SWBNNT (dashed).

In order to further analyze the water structure in the center of a large tube, Figure 15 compares the three radial distribution functions (rdf) g_{OO}, g_{OH}, and g_{HH} obtained in pure bulk water reference run with ones obtained for molecules in the center of the (20,20)-SWBNNT. Only sites inside a cylinder of 2.2 Å radius around the *z*-axis are selected as centers for these function. Since the number density ρ_b is not constant, the normalization of these functions is somewhat arbitrary. The zone of constant density inside the tube is about 8 Å wide, this case thus selected to set $g(r \approx 6\,\text{Å}) = 1$. The Figure 15 shows that all three g-functions inside the tube are almost indistinguishable from the bulk ones. Thus, even with the strongest of the three wall-water interaction models, the water inside the tube is structurally very close to bulk water.

Dynamics and diffusions of bulk water molecules and water molecules enclosed in different sizes of nanotubes

Dynamic properties of water were expressed in terms of its self-diffusion coefficient that obtained from slope of average mean square displacement (MSD) of water molecules. MSD curves show in Figure 17 (bulk system) and Figure 18 (water in confined systems).

Figure 16 shows the decay of the number of water molecules present in the boundary layer of the tube wall (defined as the water molecules with $r = \sqrt{x^2 + y^2}$ -values larger than the minima in the distribution functions shown in Figure 13(a - f) at an initial time t_0, as a function of time. This figure shows, as examples, the results for large and a small tubes and also for different interactions strengths (hydrophobicities) between water and wall. The long time limit of these functions is the expectation value of the initial molecules being present in the boundary layer when the system is totally mixed. It is seen that this value is reached in all cases after about 150 ps. Functions of type

$$f(t) = a + b * \exp(-t / \tau)$$

describe the correlation very well in all cases, the correlation times τ are all between 40 and 50 ps with the higher values for the stronger wall-water interactions. The sum $a + b$ is close to the average total number of water molecules present in the boundary layer, which is also reported in Figure 13(a-f) from integrations of the distribution functions plotted there.

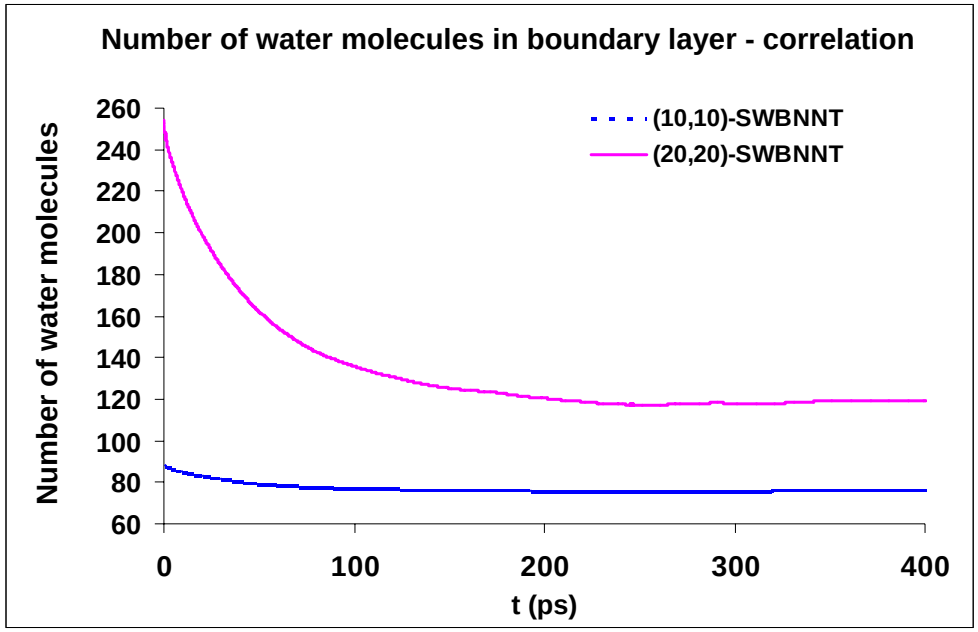

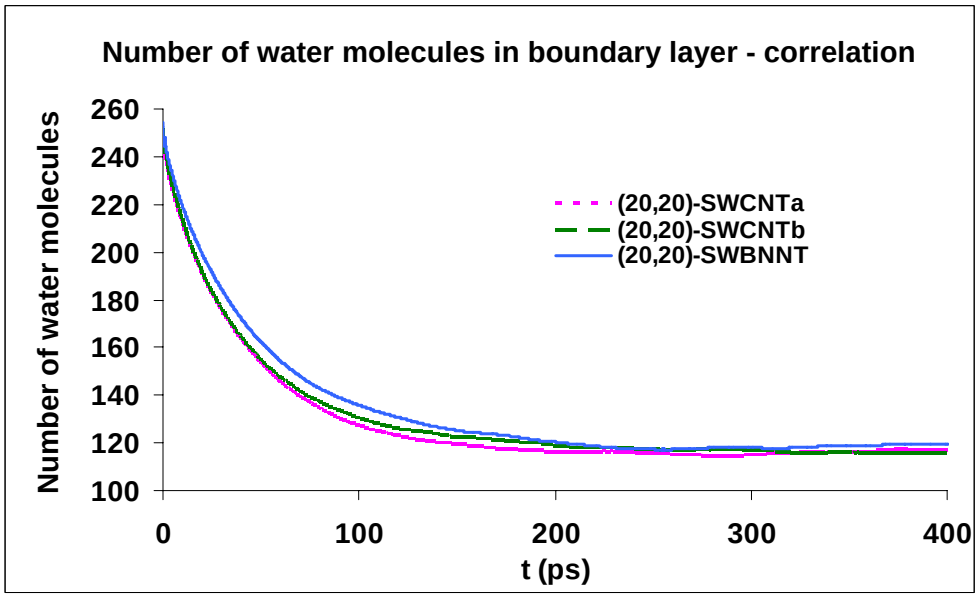

Figure 16 Average number of water molecules present in the first water layer next to the pore wall at time 0 and still present there at later times, from simulations (10,10)-SWBNNT and (20,20)-SWBNNT (*top*), and additionally, for comparison, SWCNTa and SWCNTb (*bottom*).

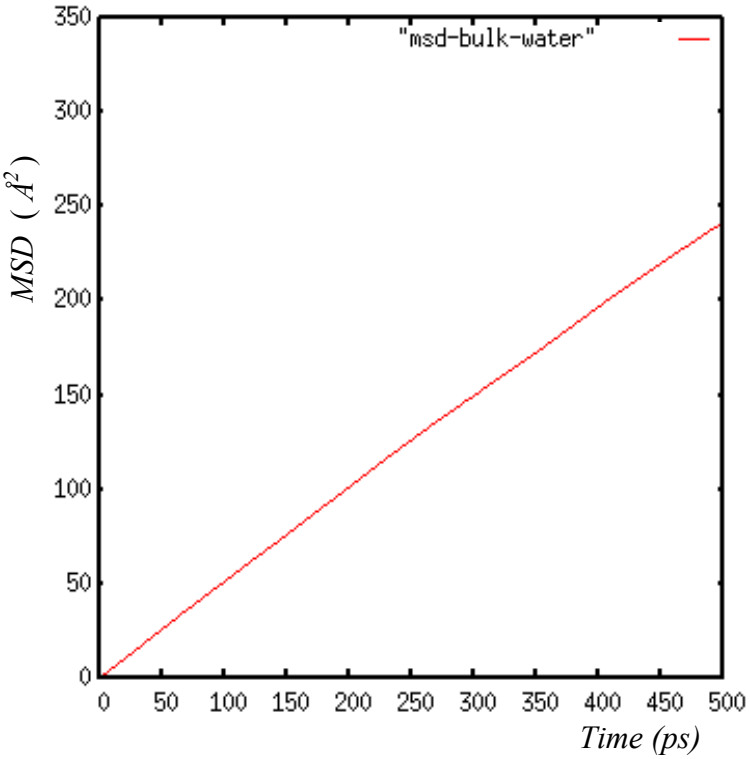

Figure 17 Axial mean square displacement (*MSD*) (z axis) of bulk water (1,000 molecules).

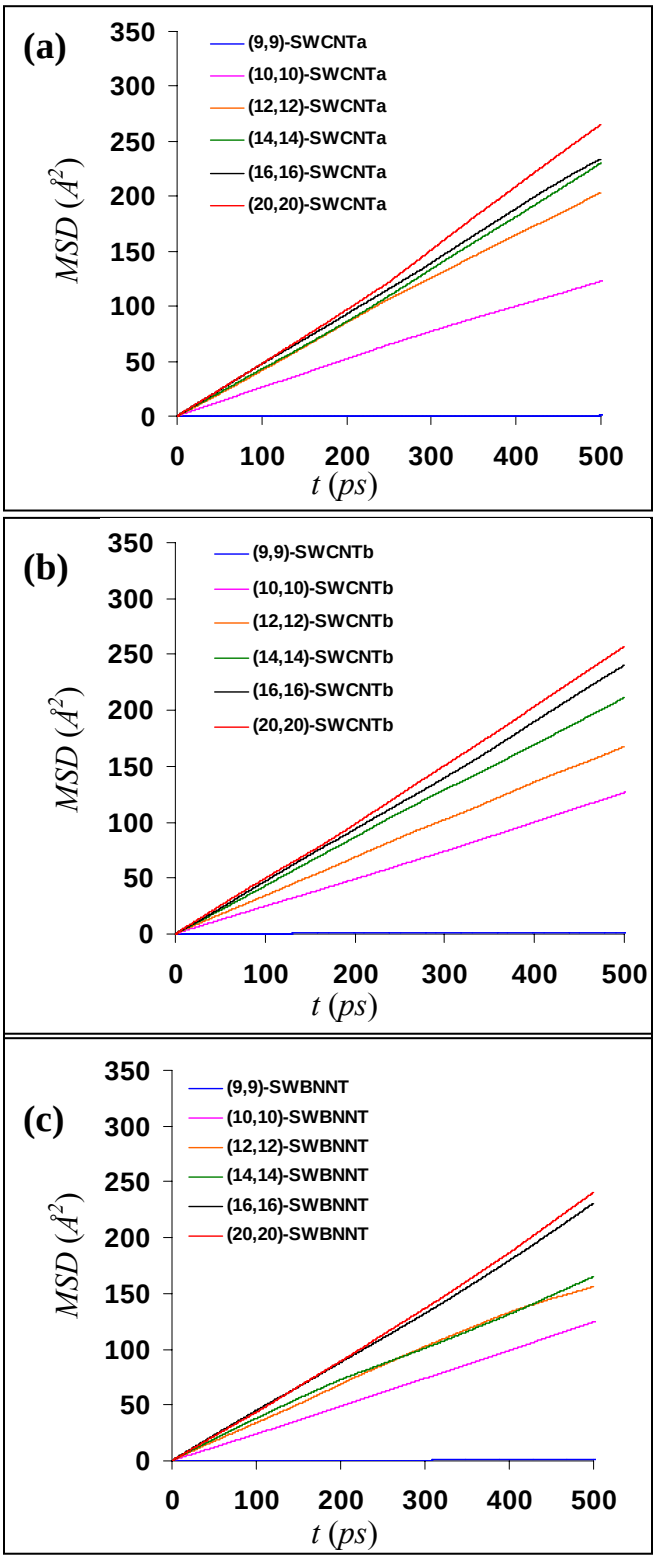

Figure 18 Mean square displacements of the oxygen atom, from simulations SWCNTa **(a)**, SWNCNTb **(b)**, and SWBNNT **(c)**. Self-diffusion coefficients see Table 5 and Figure 19.

Table 5 Axial self-diffusion coefficients ***Dz*** (cm^2/s) of water in nanotubes at the average temperature of 298 K and the water density of 1.00 g cm^{-3}. The uncertainties are estimated to be of the order of $\pm 0.10\ cm^2\ s^{-1}$

Model	***Dz*** **(**$cm^2\ s^{-1}$**)**	**Model**	***Dz*** **(**$cm^2\ s^{-1}$**)**	**Model**	***Dz*** **(**$cm^2\ s^{-1}$**)**
Bulk water	2.50×10^{-5}				
					ε_{BO}=0.11433
εij (Kcal mol^{-1})	ε_{CO}=0.11433		ε_{CO}=0.11433		ε_{NO}=0.11433
(9,9)- SWCNTa	3.00×10^{-8}	(9,9)- SWCNTb	9.80×10^{-8}	(9,9)- SWBNNT	8.55×10^{-8}
(10,10)- SWCNTa	1.20×10^{-5}	(10,10)- SWCNTb	1.30×10^{-5}	(10,10)- SWBNNT	1.50×10^{-5}
(12,12)- SWCNTa	2.05×10^{-5}	(12,12)- SWCNTb	1.70×10^{-5}	(12,12)- SWBNNT	1.60×10^{-5}
(14,14)- SWCNTa	2.30×10^{-5}	(14,14)- SWCNTb	2.10×10^{-5}	(14,14)- SWBNNT	1.60×10^{-5}
(16,16)- SWCNTa	2.35×10^{-5}	(16,16)- SWCNTb	2.40×10^{-5}	(16,16)- SWBNNT	2.40×10^{-5}
(20,20)- SWCNTa	2.70×10^{-5}	(20,20)- SWCNTb	2.60×10^{-5}	(20,20)- SWBNNT	2.50×10^{-5}

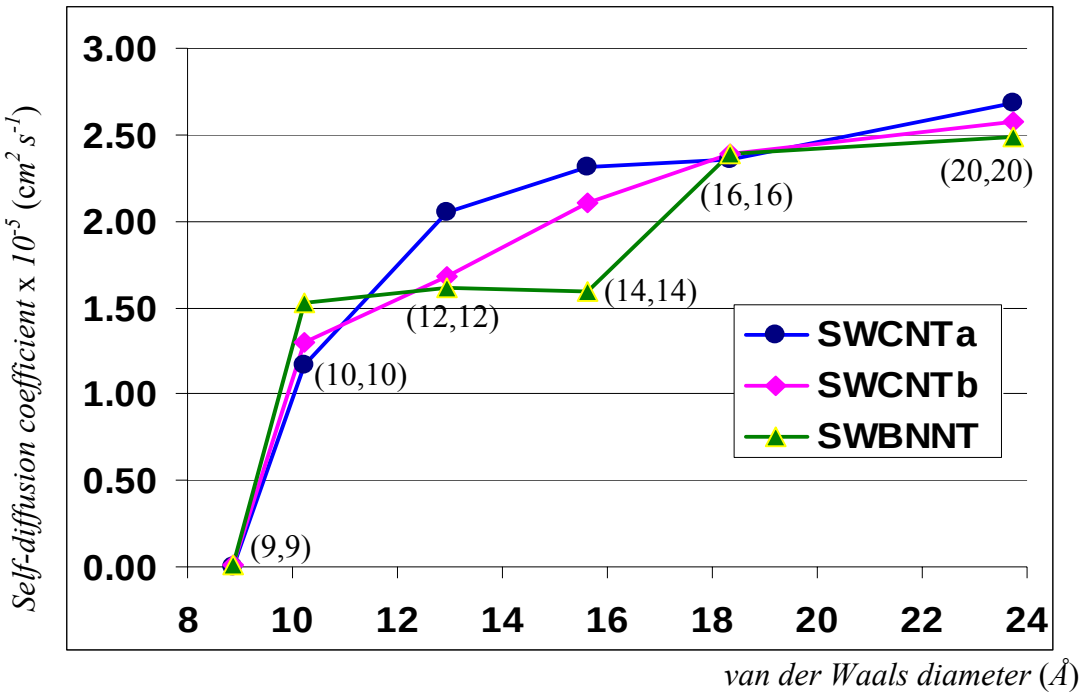

Figure 19 Comparison self-diffusion coefficients of water confined in 3 difference attractive interactions and difference size nanotube.

The Figure 18 shows the averaged mean-square displacements of the water molecules, corrected for the drifts induced by the thermostat, for all systems. The translational self-diffusion coefficients reported in Table 5 and Figure 19 have been obtained by fitting expressions

$$< (z - z_0)^2(t) >= A + 2D_z \cdot t$$

to the mean-square displacement curves in z-direction at long times. This work obtained a value of $D = 2.5 \pm 0.1 \cdot 10^{-5}$ $\mathrm{cm}^2\,\mathrm{s}^{-1}$ from the pure water simulation. This D-value is intermediate between the values reported by Marshl ($2.69 \cdot 10^{-5}\,\mathrm{cm}^2\,\mathrm{s}^{-1}$) and by experimental diffusion coefficient of water ($2.35 \cdot 10^{-5}\,\mathrm{cm}^2\,\mathrm{s}^{-1}$) (Lide, 1995). In passing, here also take good note of the remarks in these papers that the fact that the experimental D is well reproduced by a given model for the pure liquid at a given state point does not necessarily mean that it will also do so in solutions, at an interface, or under different thermodynamic conditions. This work nevertheless expects systematic trends (e.g. size dependences, or when the wall-water interactions are modified) to be reasonably well mirrored.

Figure 19 shows that no self-diffusion can be detected in the narrowest tubes during the simulation runs of a few nanoseconds. D_z increases with increasing tube diameter and reaches its bulk value in the widest tubes with diameters of about 24 Å, the convergence being faster for smaller wall-water interactions. In the case of the boron-nitride tubes the convergence is not monotonous. These systems were not able to distinguish particular structural features that may explain the plateau between (10,10) and (14,14) tubes (which here is outside uncertainties) in a convincing way. Even larger irregular variations of the self-diffusion have been observed by Liu *et al.* (Liu *et al.*, 2005) in narrower CNTs. No influence of the wall-water interactions can be distinguished in tubes wider than about 20 Å.

It is seen in Figure 19 that in almost all cases the linear regime of the mean-square displacement is reached after about 10 ps. Comparing this time with the correlation time for water molecules staying in the boundary layer discussed above (see Figure 16), viz. about 40 to 50 ps, indicates that a separation of the total diffusion into a component originating in the boundary layer molecules and a second one originating in the bulk would be justified.

In all cases, the self-diffusion coefficients increase as the nanotube diameters increase. In the case of the small diameter (9,9) nanotubes, the water shows anomalous ice-like behavior in both ice coordination number and very slow flow of 3 order less than that seen in bulk and the large-nanotubes, while a liquid-like degree of water-water hydrogen bonding.

For the wider pore (12,12), (14,14), (16,16) and (20,20) nanotubes, the axial self-diffusion coefficients increase as the pore increase and reach that to the bulk water. The diffusion is sensitive to the $\varepsilon_{C\text{-}O}$ van der Waals attractive interaction (LJ potential). The simulations of water in SWCNTa and SWCNTb represented the smooth attractive interactions; the small energy interaction ($\varepsilon c\text{-}o$ = 0.1143 kcal mol^{-1}) gives the large self-diffusion coefficients while the higher interaction ($\varepsilon c\text{-}o$ = 0.1230 kcal mol^{-1}) gives smaller self-diffusion coefficients.

CONCLUSIONS

MD simulations were used to study the molecular distributions and transport properties of water confined in nanotubes with difference of pore diameters and attractive interactions between wall and water. Water motions and orientations can be modified by confining in single-walled nanotubes. In the (9,9)-armchair nanotubes, water adopts a six-membered ring ice-like structure. The distribution structure of water confined in nano-space is not homogeneous. The larger diameter nanotubes, multi-layering of water occur, where water behaves like bulk water in the inner layers. Water molecules can freely exchange between inner and outer layers. Self-diffusion coefficient of water increases as the nanotube diameter increases. The attractive interactions between water and nanotube wall is a key role of water diffusivity. Small changes in the water-wall interaction can lead to changes in the axial diffusion of water in nanotubes at identical sizes. The axial diffusion of water in the SWCNTa and SWCNTb are faster than that in the SWBNNT ((12,12)-(20,20)-nanotubes), the strong attractive interactions (water and tube wall) impose the slower diffusion of water.

LITERATURE CITED

Bai, J., J. Wang and X.C. Zeng. 2006. Multiwalled ice helixes and ice nanotubes. **Proceedings of the National Academy of Sciences of the United States of America** 103(52):19664-19667.

Behler, J., D.W. Price and M.G.B. Drew. 2001. Water structuring properties of carbohydrates, molecular dynamics studies on 1,5-anhydro-D-fructose. **Physical Chemistry Chemical Physics** 3(4):588-601.

Berendsen, H.J.C., J.R. Grigera and T.P. Straatsma. 1987. The missing term in effective pair potentials. **Journal of Physical Chemistry** 91(24):6269-6271.

Berezhkovskii, A. and G. Hummer. 2002. Single-File Transport of Water Molecules through a Carbon Nanotube. **Physical Review Letters** 89(6):064503/064501-064503/064504.

Bianco, A., K. Kostarelos and M. Prato. 2005. Applications of carbon nanotubes in drug delivery. **Current Opinion in Chemical Biology** 9(6):674-679.

Chou, C.-C., H.-Y. Hsiao, Q.-S. Hong, C.-H. Chen, Y.-W. Peng, H.-W. Chen and P.-C. Yang. 2008. Single-Walled Carbon Nanotubes Can Induce Pulmonary Injury in Mouse Model. **Nano Letters** 8(2):437-445.

Golberg, D., Y. Bando, K. Kurashima and T. Sato. 2000. MoO3-promoted synthesis of multi-walled BN nanotubes from C nanotube templates. **Chemical Physics Letters** 323(1,2):185-191.

Guillot, B. 2002. A Reappraisal of what we have learnt during three decades of computer simulations on water. **Journal of Molecular Liquids** 101(1-3):219-260.

Head-Gordon, T. and M.E. Johnson. 2006. Tetrahedral structure or chains for liquid water. **Proceedings of the National Academy of Sciences of the United States of America** 103(21):7973-7977.

Hummer, G., J.C. Rasaiah and J.P. Noworyta. 2001. Water conduction through the hydrophobic channel of a carbon nanotube. **Nature** 414(6860):188-190.

Iijima, S. 1991. Helical microtubules of graphitic carbon. **Nature** 354(6348):56-58.

Iijima, S. and T. Ichihashi. 1993. Single-shell carbon nanotubes of 1-nm diameter. **Nature** 363:603-605.

Ishigami, M., S. Aloni and A. Zettl. 2003a. Properties of boron nitride nanotubes. **American Institute of Physics Conference Proceedings** 696 (Scanning Tunneling Microscopy/Spectoscopy and Related Techniques):94-99.

Ishigami, M., S. Aloni and A. Zettl. 2003b. Scanning tunneling microscopy and spectroscopy of boron nitride nanotubes. **American Institute of Physics Conference Proceedings Conference Proceedings** 685 (Molecular Nanostructures):389-393.

Joseph, S. and N.R. Aluru. 2008. Why Are Carbon Nanotubes Fast Transporters of Water? **Nano Letters** 8(2):452-458.

Kalra, A., S. Garde and G. Hummer. 2003. Osmotic water transport through carbon nanotube membranes. **Proceedings of the National Academy of Sciences of the United States of America** 100(18):10175-10180.

Kalra, A., G. Hummer and S. Garde. 2004. Methane Partitioning and Transport in Hydrated Carbon Nanotubes. **Journal of Physical Chemistry B** 108(2):544-549.

Koga, K., G.T. Gao, H. Tanaka and X.C. Zeng. 2001. Formation of ordered ice nanotubes inside carbon nanotubes.**Nature** 412(6849):802-805.

Koga, K., R.D. Parra, H. Tanaka and X.C. Zeng. 2000a. Ice nanotube: What does the unit cell look like? **Journal of Chemical Physics** 113(12):5037-5040.

Koga, K. and H. Tanaka. 2005. Phase diagram of water between hydrophobic surfaces. **Journal of Chemical Physics** 122(10):104711.

Koga, K., H. Tanaka and X.C. Zeng. 2000b. First-order transition in confined water between high-density liquid and low-density amorphous phases. **Nature** 408(6812):564-567.

Kolesnikov, A.I., J.-M. Zanotti, C.-K. Loong, P. Thiyagarajan, A.P. Moravsky, R.O. Loutfy and C.J. Burnham. 2004. Anomalously Soft Dynamics of Water in a Nanotube: A Revelation of Nanoscale Confinement. **Physical Review Letters** 93(3):035503/035501-035503/035504.

Kuhs, W.F., J.L. Finney, C. Vettier and D.V. Bliss. 1984. Structure and hydrogen ordering in ices VI, VII, and VIII by neutron powder diffraction. **Journal of Chemical Physics** 81(8):3612-3623.

Li, J., X. Gong, H. Lu, D. Li, H. Fang and R. Zhou. 2007. Electrostatic gating of a nanometer water channel. **Proceedings of the National Academy of Sciences of the United States of America** 104(10):3687-3692.

Li, L., D. Bedrov and G.D. Smith. 2006. Water-Induced Interactions between Carbon Nanoparticles. **Journal of Physical Chemistry B** 110(21):10509-10513.

Lide, D. R., Ed. 1995. **Handbook of Chemistry and Physics.** CRC Boca Raton, FL.

Liu, Y. and S. Consta. 2005. Dynamic breaking and restoring of finite water chains inside carbon nanotubes. **Computing Letters** 1(4):192-197.

Liu, Y. and Q. Wang. 2005. Transport behavior of water confined in carbon nanotubes. **Physical Review B: Condensed Matter and Materials Physics** 72(8):085420/085421-085420/085424.

Liu, Y., Q. Wang, T. Wu and L. Zhang. 2005a. Fluid structure and transport properties of water inside carbon nanotubes. **Journal of Chemical Physics** 123(23):234701/234701-234701/234707.

Liu, Y., Q. Wang, L. Zhang and T. Wu. 2005b. Dynamics and Density Profile of Water in Nanotubes as One-Dimensional Fluid. **Langmuir** 21(25):12025-12030.

Malek, K. and M.-O. Coppens. 2003. Knudsen self- and Fickian diffusion in rough nanoporous media. **Journal of Chemical Physics** 119(5):2801-2811.

Mann, D.J. and M.D. Halls. 2003. Water Alignment and Proton Conduction inside Carbon Nanotubes. **Physical Review Letters** 90(19):195503/195501-195503/195504.

Marti, J. and M.C. Gordillo. 2001a. Temperature effects on the static and dynamic properties of liquid water inside nanotubes. **Physical Review E: Statistical, Nonlinear, and Soft Matter Physics** 64(2-1):021504/021501-021504/021506.

Marti, J. and M.C. Gordillo. 2001b. Time-dependent properties of liquid water isotopes adsorbed in carbon nanotubes. **Journal of Chemical Physics** 114(23):10486-10492.

Marti, J. and M.C. Gordillo. 2002. Microscopic dynamics of confined supercritical water. **Chemical Physics Letters** 354(3,4):227-232.

Marti, J. and M.C. Gordillo. 2003. Structure and dynamics of liquid water adsorbed on the external walls of carbon nanotubes. **Journal of Chemical Physics** 119(23):12540-12546.

Mashl, R.J., S. Joseph, N.R. Aluru and E. Jakobsson. 2003. Anomalously Immobilized Water: A New Water Phase Induced by Confinement in Nanotubes. **Nano Letters** 3(5):589-592.

Meyyappan, M., Ed. 2005. **Carbon nanotubes: Science and applications**. Boca Raton, CRC Press LLC

Mukherjee, B., P.K. Maiti, C. Dasgupta and A.K. Sood. 2007a. Strong correlations and Fickian water diffusion in narrow carbon nanotubes. **Journal of Chemical Physics** 126(12):124704/124701-124704/124708.

Mukherjee, B., K. Maiti Prabal, C. Dasgupta and A.K. Sood. 2007b. Structure and dynamics of confined water inside narrow carbon nanotubes. **Journal of Nanoscience and Nanotechnology** 7(6):1796-1799.

Noy, A., H.G. Park, F. Fornasiero, J.K. Holt, C.P. Grigoropoulos and O. Bakajin. 2007. Nanofluidics in carbon nanotubes. **Nano Today** 2(6):22-29.

Smith, W.T. R. Forester, I. T. Todorov and M. Leslie. 2006. The DL_POLY 2.0, User Manual, CCLRC, Daresbury Laborator Daresbury, UK, Version 2.17.

Soper, A.K. 2000. The radial distribution functions of water and ice from 220 to 673 K and at pressures up to 400 MPa. **Chemical Physics** 258(2-3):121-137.

Striolo, A. 2006. The Mechanism of Water Diffusion in Narrow Carbon Nanotubes. **Nano Letters** 6(4):633-639.

Striolo, A., A.A. Chialvo, P.T. Cummings and K.E. Gubbins. 2003. Water Adsorption in Carbon-Slit Nanopores. **Langmuir** 19(20):8583-8591.

Striolo, A., A.A. Chialvo, P.T. Cummings and K.E. Gubbins. 2006. Simulated water adsorption in chemically heterogeneous carbon nanotubes. **Journal of Chemical Physics** 124(7):074710/074711-074710/074711.

Striolo, A., P.T. Cummings, A.A. Chialvo and K.E. Gubbins. 2004a. Adsorption and diffusion of water in activated carbon nanopores. **Advances in Science and Technology (Faenza, Italy)** 42 (Computational Modeling and Simulation of Materials III, Part A):531-540.

Striolo, A., K.E. Gubbins, A.A. Chialvo and P.T. Cummings. 2004b. Simulated water adsorption isotherms in carbon nanopores. **Molecular Physics** 102(3):243-251.

Sui, H., B.G. Han, J.K. Lee, P. Walian and B.K. Jap. 2001. Structural basis of water-specific transport through the AQP1 water channel. **Nature** 414(6866):872-878.

Supple, S. and N. Quirke. 2003. Rapid Imbibition of Fluids in Carbon Nanotubes. **Physical Review Letters** 90(21):214501/214501-214501/214504.

Supple, S. and N. Quirke. 2004. Molecular dynamics of transient oil flows in nanopores I: imbibition speeds for single wall carbon nanotubes. **Journal of Chemical Physics** 121(17):8571-8579.

Supple, S. and N. Quirke. 2005. Molecular dynamics of transient oil flows in nanopores. Part 2. Density profiles and molecular structure for decane in carbon nanotubes. **Journal of Chemical Physics** 122(10):104706/104701-104706/104708.

Tajkhorshid, E., P. Nollert, O. Jensen Morten, J.W. Miercke Larry, J. O'Connell, M. Stroud Robert and K. Schulten. 2002. Control of the selectivity of the aquaporin water channel family by global orientational tuning. **Science** 296(5567):525-530.

Takaiwa, D., K. Koga and H. Tanaka. 2007. Structures of filled ice nanotubes inside carbon nanotubes. **Molecular Simulation** 33(1-2):127-132.

Waghe, A., J.C. Rasaiah and G. Hummer. 2002. Filling and emptying kinetics of carbon nanotubes in water. **Journal of Chemical Physics** 117(23):10789-10795.

Wang, Z.L., P. Poncharal and W.A. De Heer. 2000. Measuring physical and mechanical properties of individual carbon nanotubes by in situ TEM. **Journal of Physics and Chemistry of Solids** 61(7):1025-1030.

Won, C.Y. and N.R. Aluru. 2007. Water Permeation through a Subnanometer Boron Nitride Nanotube. **Journal of the American Chemical Society** 129(10):2748-2749.

Won, C.Y. and N.R. Aluru. 2008. Structure and Dynamics of Water Confined in a Boron Nitride Nanotube. **Journal of Physical Chemistry C** 112(6):1812-1818.

Yang, L. and S. Garde. 2007. Modeling the selective partitioning of cations into negatively charged nanopores in water. **Journal of Chemical Physics** 126(8):084706/084701-084706/084708.

Zou, J., B. Ji, X.-Q. Feng and H. Gao. 2006a. Molecular-dynamic studies of carbon-water-carbon composite nanotubes. **Small** 2(11):1348-1355.

Zou, J., B. Ji, X.-Q. Feng and H. Gao. 2006b. Self-Assembly of Single-Walled Carbon Nanotubes into Multiwalled Carbon Nanotubes in Water: Molecular Dynamics Simulations. **Nano Letters** 6(3):430-434.

APPENDICES

Appendix A

Data support

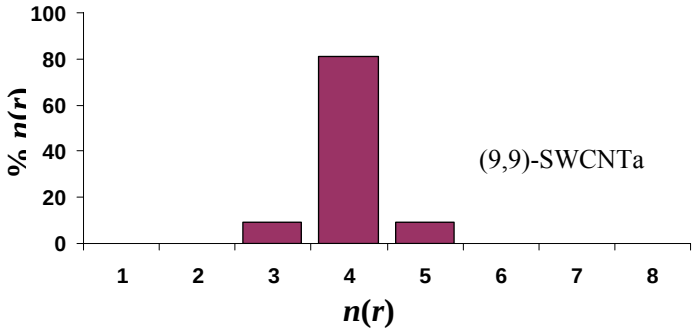

(a) water 77 molecules in (9,9)-SWCNTa

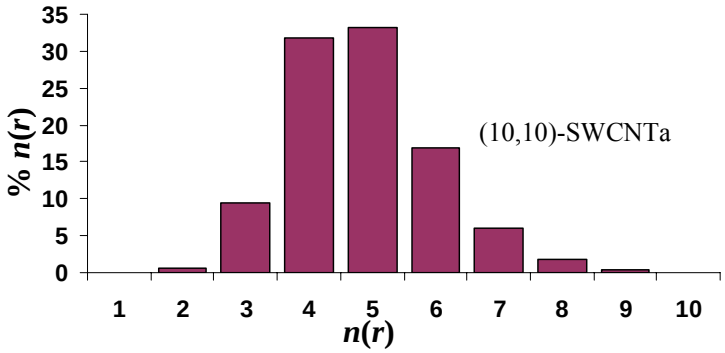

(b) water 102 molecules in (10,10)-SWCNTa

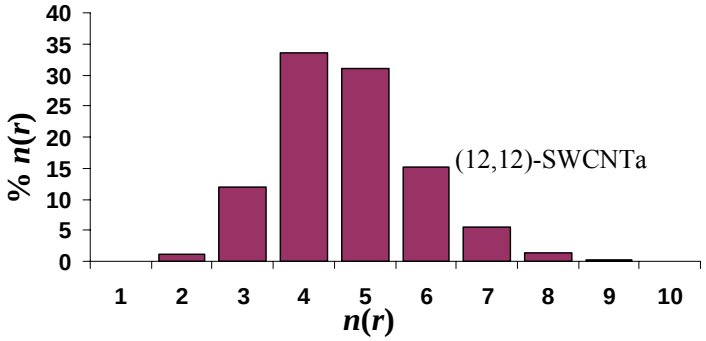

(c) water 162 molecules in (12,12)-SWCNTa

Figure A1 Histogram of coordination number distribution of water in SWCNTa ε_{co} = *0.114333* kcal mol^{-1}.

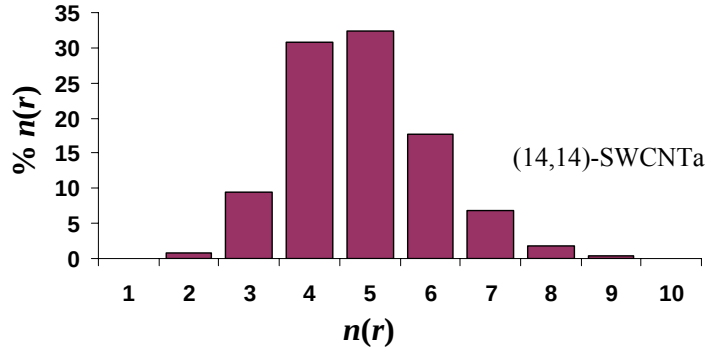

(d) water 237 molecules in (14,14)-SWCNTa

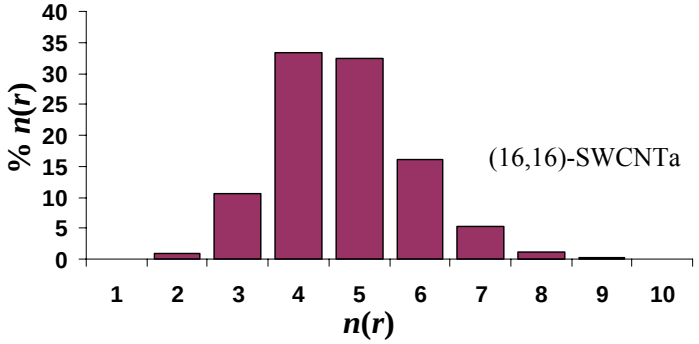

(e) water 327 molecules in (16,16)-SWCNTa

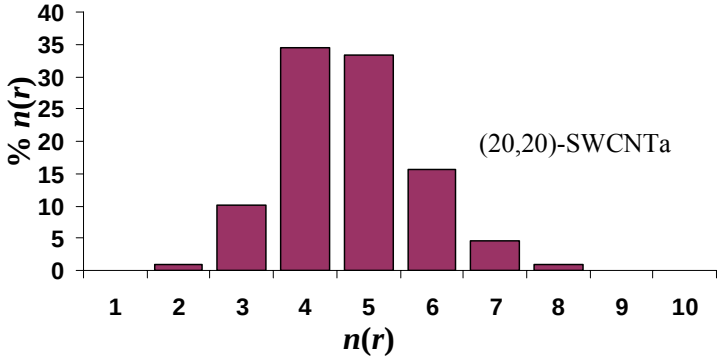

(f) water 547 molecules in (20,20)-SWCNTa

Figure A1 Histogram of coordination number distribution of water in SWCNTa ε_{co} = *0.114333 kcal* mol^{-1}. (cont'd)

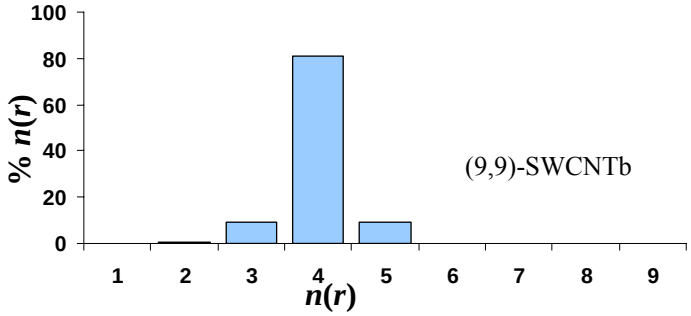

(a) water 77 molecules in (9,9)-SWCNTb

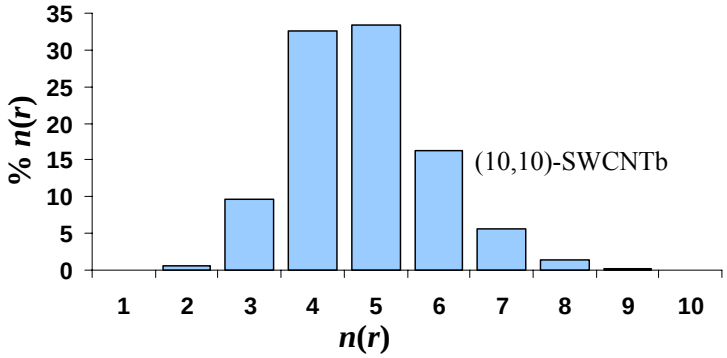

(b) water 102 molecules in (10,10)-SWCNTb

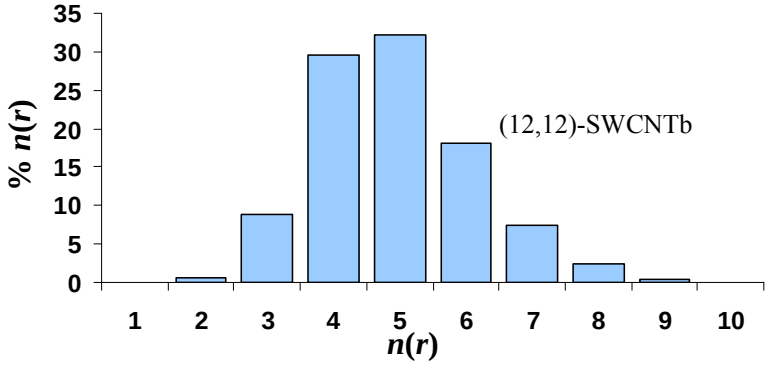

(c) water 162 molecules in (12,12)-SWCNTb

Figure A2 Histogram of coordination number distribution of water in SWCNTb ε_{co} = *0.12300* kcal mol^{-1} .

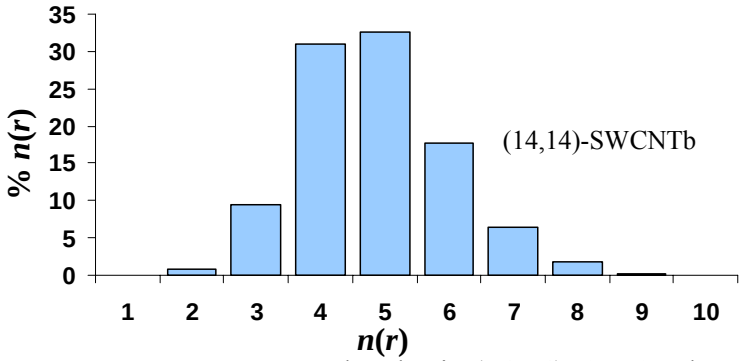

(d) water 237 molecules in (14,14)-SWCNTb

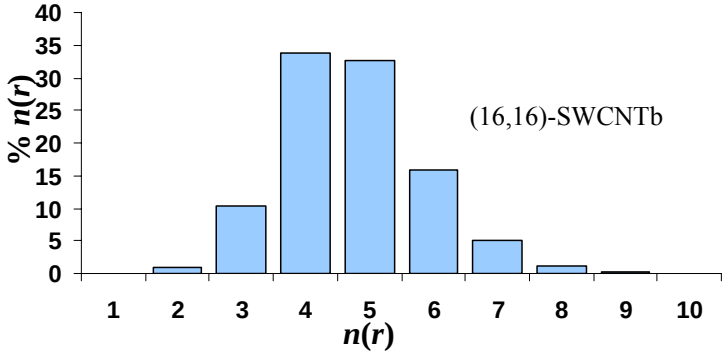

(e) water 327 molecules in (16,16)-SWCNTb

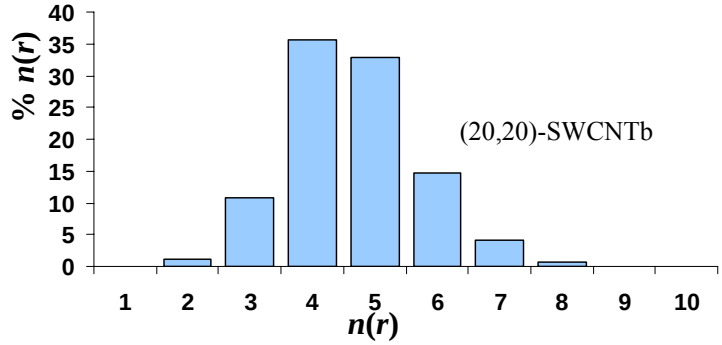

(f) water 547 molecules in (20,20)-SWCNTb

Figure A2 Histogram of coordination number distribution of water in SWCNTb ε_{co} = *0.12300* kcal mol^{-1} .

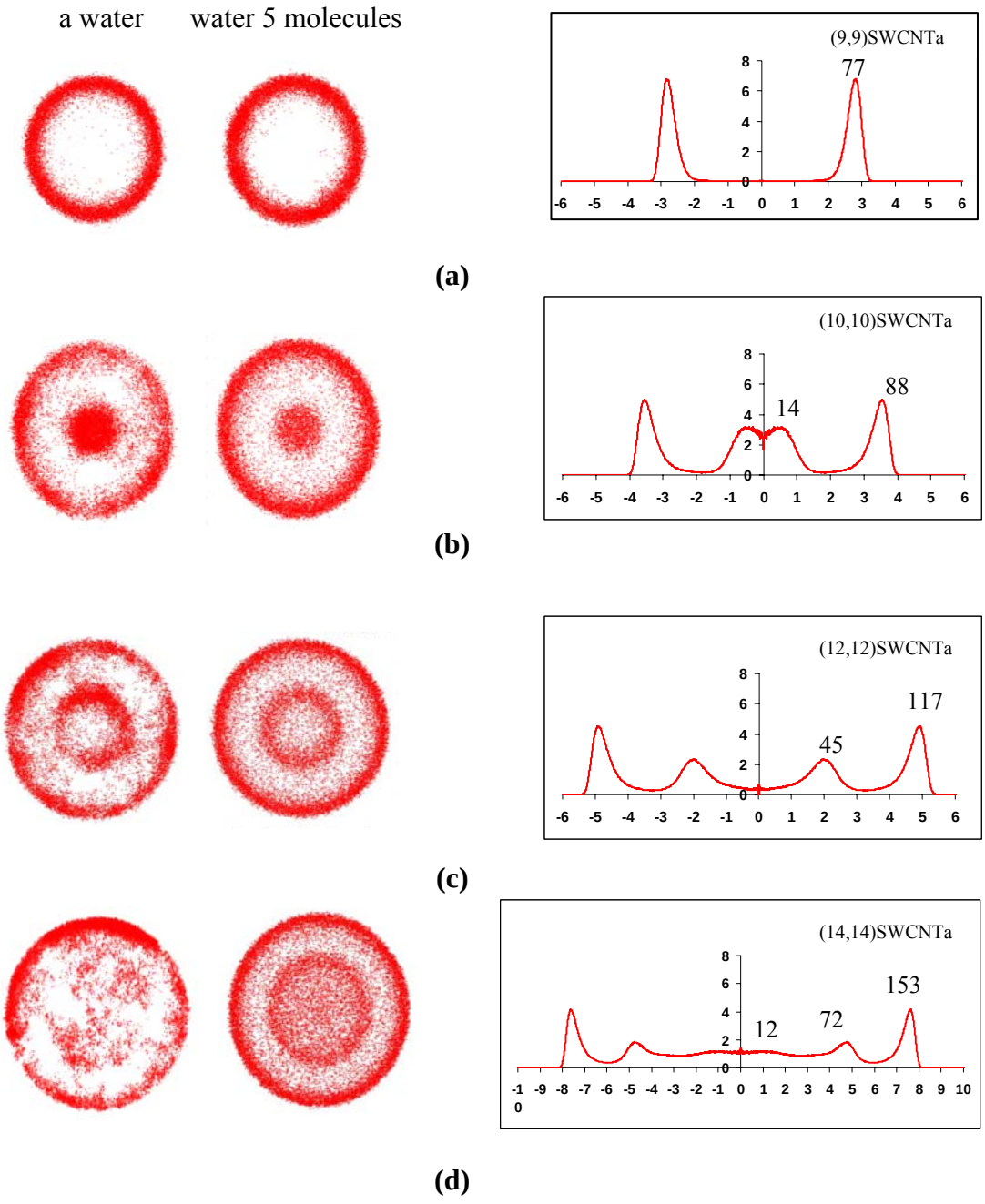

Figure A3 Cylindrical $g(r)$-function (*right*) of the water and trajectory plot of 1 (*left*) and 5 (*middle*) water molecules for the simulation of the (9,9)-**(a)**, (10,10)-**(b)**, (12,12)-**(c)**, (14,14)-**(d)**, (16,16)-**(e)** and (20,20)-**(f)** armchair SWCNTa (ε_{O-C} = *0.11433* kcal mol^{-1})

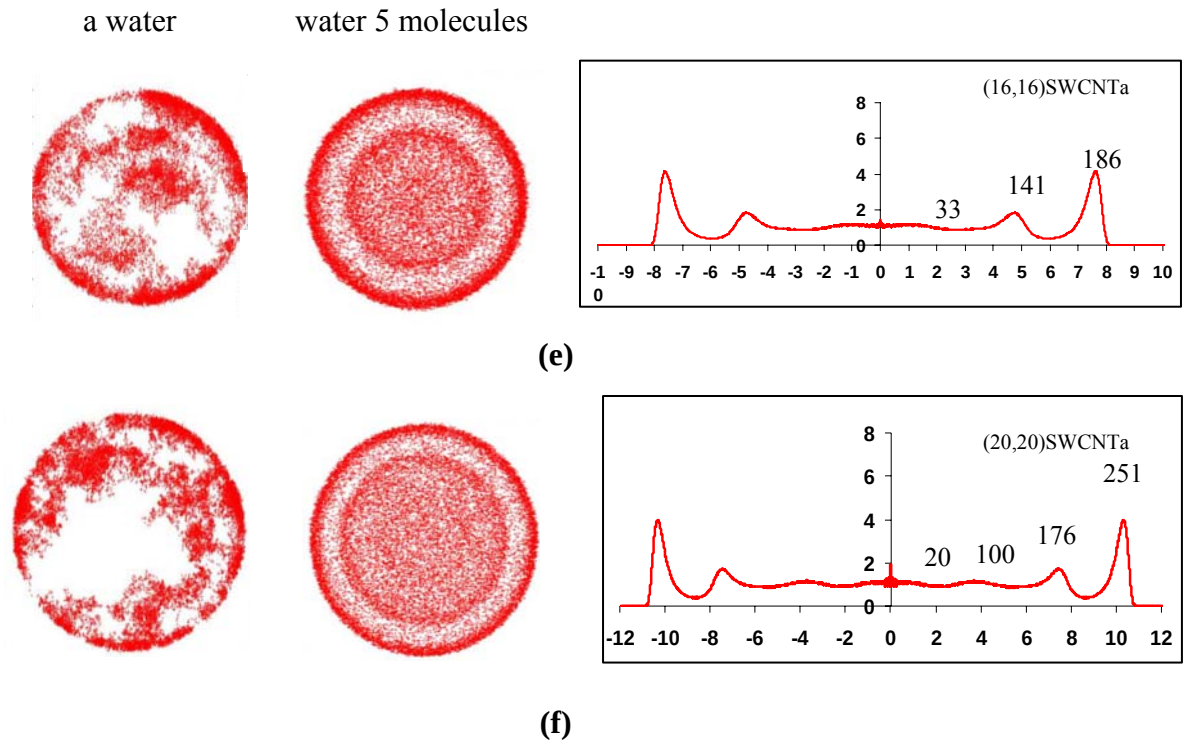

Figure A3 Cylindrical $g(r)$-function (*right*) of the water and trajectory plot of 1 (*left*) and 5 (*middle*) water molecules for the simulation of the (9,9)-**(a)**, (10,10)-**(b)**, (12,12)-**(c)**, (14,14)-**(d)**, (16,16)-**(e)** and (20,20)-**(f)** armchair SWCNTa (ε_{O-C} = *0.11433* kcal mol^{-1}). (cont'd)

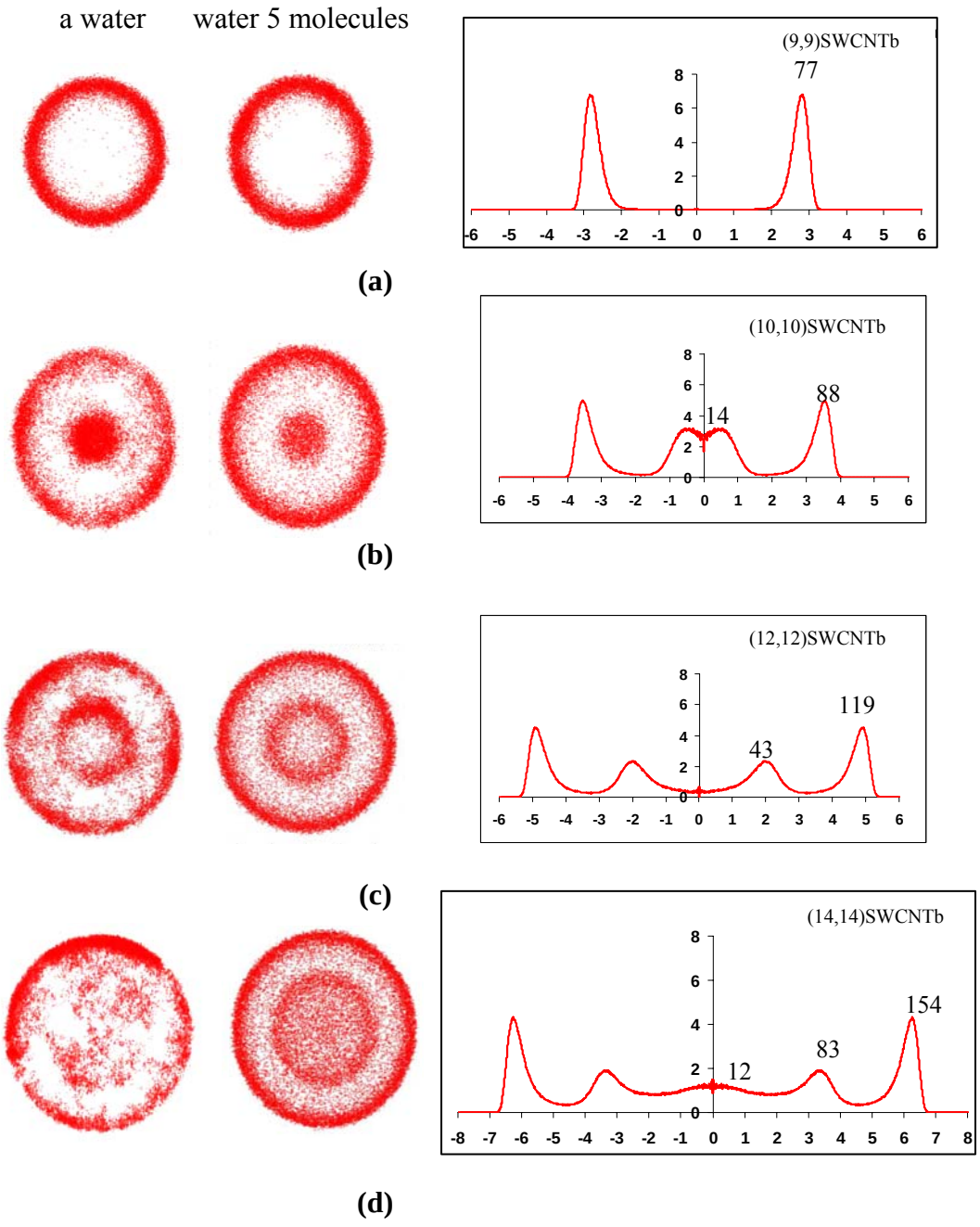

Figure A4 Cylindrical $g(r)$-function (*right*) of the water and trajectory plot of 1 (*left*) and 5 (*middle*) water molecules for the simulation of the (9,9)-**(a)**, (10,10)-**(b)**, (12,12)-**(c)**, (14,14)-**(d)**, (16,16)-**(e)** and (20,20)-**(f)** armchair SWCNTb (ε_{O-C} = *0.12300* kcal mol^{-1})

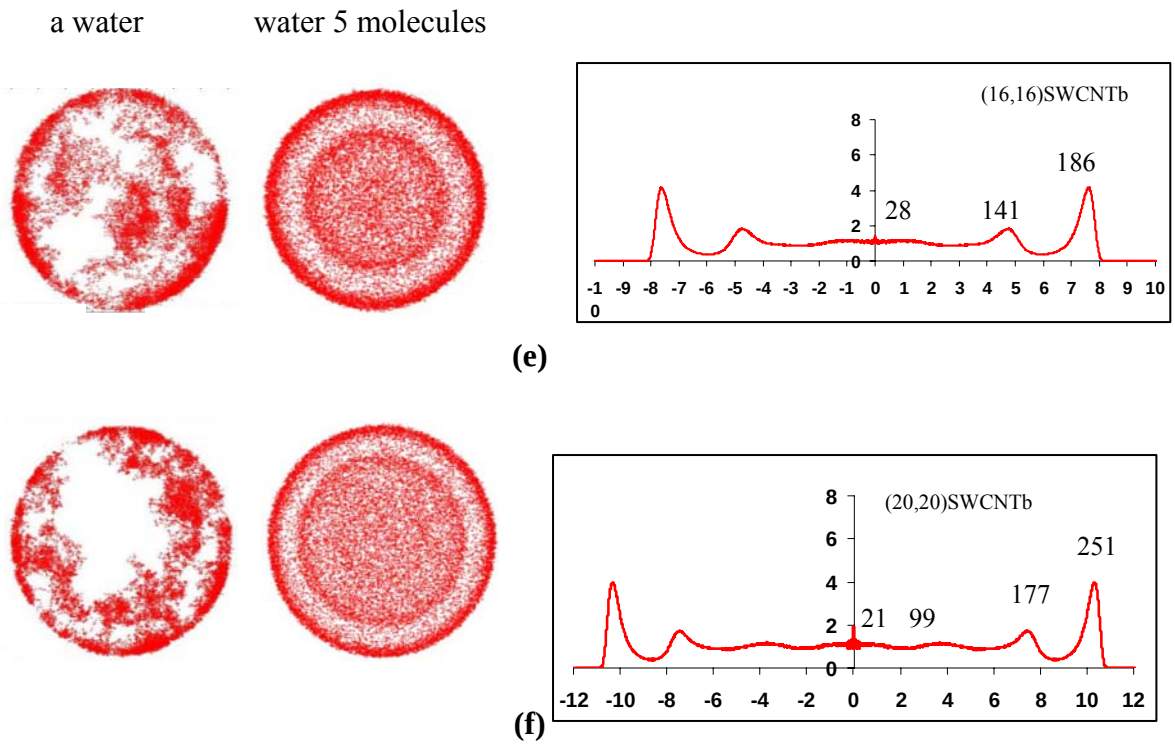

Figure A4 Cylindrical $g(r)$-function (*right*) of the water and trajectory plot of 1 (*left*) and 5 (*middle*) water molecules for the simulation of the (9,9)-**(a)**, (10,10)-**(b)**, (12,12)-**(c)**, (14,14)-**(d)**, (16,16)-**(e)** and (20,20)-**(f)** armchair SWCNTb ($\varepsilon_{O-C} = 0.12300$ kcal mol^{-1}).(cont'd)

Appendix B

Curriculum vitae and presentations

CURRICULUM VITAE

NAME : Miss Nongnuch Artrith

BIRTH PLACE : Maha Sarakham, Thailand

NATIONALITY : Thai

EDUCATION : 1997-2001, Khon Kaen University, B.Sc. (Physics)

SCHOLARSHIPS / AWARDS:

1. Thailand Research Fund (to JL)
2. Kasetsart University Research and Development Institute (KURDI)
3. National Nanotechnology Center (NANOTEC center of Excellence and Computational Nanoscience Consortium)
4. National Research Council of Thailand (NRCT)
5. Commission on Higher Education (Postgraduate Education and Research Programs in Petroleum, and Petrochemicals, and Advanced Materials and Postdoctoral Research Grants to TN), Ministry of Education
6. Graduate School Kasetsart University Fund
7. Research Assistant Scholarship, Kasetsart University
8. Innovative Leadership Award from National Science and Technology Development Agency (NSTDA), January 20-22, 2006.

(http://www.nstda.or.th/hrd/permanentcamp/activity/2006/leadercamp/index.html)

CONFERENCES / PRESENTATIONS:

a. **Molecular Dynamics Simulation Studies of Water Confined in SWCNTs and SWBNNTs.** (poster presentation)

Nongnuch Artrith, Tanin Nanok, Piboon Puntu and Jumras Limtrakul. Abstract of papers Congress on Pure and Applied Chemistry International Conference (PACCON 2008) January 30 - February 1, **2008**, 144.

b. **Structure and dynamics properties of water Confined in Nanotubes(CNTs and BNNTs) : A Molecular Dynamics Study**. (Oral presentation)

Nongnuch Artrith, Tanin Nanok, Piboon Puntu and Jumras Limtrakul. Proceeding of papers 33rd Congress on Science and Technology of Thailand (STT33), Walailak University, Thailand, October 18-20, **2007**, 199.

c. **The influence of -CH_3, -C_6H_5, -F, and –Carbon nanotubes on the hydrogen-bonded Adenine / Thymine adduct.** (Poster presentation)

Montree Sawangphruk, **Nongnuch Artrith,** Pipat Khongpracha and Jumras Limtrakul. Abstracts of Papers, 231st Congress on American Chemical Society National Meeting, Atlanta, GA, United States, March 26-30, **2006**, and oral presentation in 33rd Congress on Science and Technology of Thailand (STT31), Suranaree Universit of Technology, Thailand, October 18-20, **2005.**

Molecular Dynamics Simulation Studies of Water Confined in SWCNTs and SWBNNTs

Nongnuch Artrith[1, 2], Tanin Nanok[1, 2, 3], Piboon Pantu[1, 2, 3], Jumras Limtrakul [1, 2, 3]*

[1]*Laboratory for Computational and Applied Chemistry, Department of Chemistry, Faculty of Science, Kasetsart University, Bangkok 10900, Thailand*
[2]*Center of Nanotechnology, Kasetsart University Research and Development Institute, Kasetsart University, Bangkok 10900, Thailand*
[3]*NANOTEC Center of Excellence, National Nanotechnology Center, Kasetsart University, Bangkok 10900, Thailand*
**E-mail: jumras.l@ku.ac.th, Tel.662-562555 ext 2159, Fax 662-5625555 ext 2176*

Diffusion and molecular distribution of water confined in nanopores are important aspects for attaining scientific and technological features in the biological micro-fluidic systems. Here, we report the structure and dynamic properties of water confined in nanotubes using molecular dynamics (MD) simulations. The water density of 1.00 g/cm^3 was placed inside the periodic models of the (*n*,*n*)-armchair nanotubes (where *n* = 9, 12, 14, 16 and 20) for single-walled carbon nanotubes (SWCNTs) and boron nitride nanotubes (SWBNNTs) at the average temperature of 298 K. It was found that the confinement effect of narrow-pore nanotubes has a strong influence on both the molecular distribution and transport phenomena. Water molecules form the ice-like single-shell hexagonal structure inside the (9,9)-armchair SWCNT and SWBNNT, while multi-layered cylindrical structures are observed in larger nanotubes. In the largest studied nanotubes (20,20), water molecules can freely exchange between inner layers. The diffusion of water molecules through the (9,9)-SWBNNTs is twice faster than through the (9,9)-SWCNTs. This is due to the stronger van der Waals interaction between water and boron nitride nanotubes. The difference in diffusion rates between two types of nanotubes becomes small when the nanotube diameter increases.

REFERENCES

1. Tajkhorshid, E.; Nollert, P.; Jensen, M.; Miercke, L. J. W.; O'Connell, J.; Stroud, R. M.; Schulten, K. *Science*. **2002,** 296, 525-530.
2. Mashl, R. J.; Joseph, S.; Aluru, N. R.; Jakobsson, E. *Nano Lett*. **2003**, 3, 589-592.
3. Liu, Y.; Wang, Q.; Zhang L.; Wu, T. *J. Langmuir*. **2005**, 21, 12025-12030.
4. Liu, Y.; Wang, Q.; Wu. T., Zhang, L. *J. Chem. Phys*. **2005,** 123, 234701-234707.
5. Won, C. Y.; Aluru, N. R. *J. Am Chem. Soc*. **2007**, 129, 2748-2749.

ACKNOWLEDGEMENT

This work was supported in part by grants from the Thailand Research Fund (to JL) and the Kasetsart University Research and Development Institute (KURDI), the National Nanotechnology Center (NANOTEC center of Excellence and Computational Nanoscience Consortium), the National Research Council of Thailand (NRCT) and the Commission on Higher Education (Postgraduate Education and Research Programs in Petroleum, and Petrochemicals, and Advanced Materials and Postdoctoral Research Grants to TN), Ministry of Education. The support from the Graduate School Kasetsart University is also acknowledged.

การศึกษาสมบัติเชิงโครงสร้างและเชิงพลวัตของน้ำในท่อนาโนทิวบ์ โดยระเบียบวิธี Molecular Dynamics

STRUCTURE AND DYNAMIC PROPERTIES OF WATER CONFINED IN NANOTUBES: A MOLECULAR DYNAMICS STUDY

นงค์นุช อาจฤทธิ์[1,2], ธานิน นานอก[1,2], พิบูลย์ พันธุ[1,2], จำรัส ลิ้มตระกูล[1,2*]
Nongnuch Artrith[1,2], Tanin Nanok[1,2], Piboon Puntu[1,2], Jumras Limtrakul[1,2*]

[1] Physical Chemistry Division, Department of Chemistry, Faculty of Science, Kasetsart University, Bangkok 10900, Thailand
[2]Center of Nanotechnology, Kasetsart University Research and Development Institute, Bangkok 10900, Thailand
[*]Corresponding author: Tel. 662-294289000 ext 304, Fax 662-5625555 ext 2176, E-mail: jumras.l@ku.ac.th

บทคัดย่อ: การใช้ระเบียบวิธี Molecular Dynamics ศึกษาสมบัติเชิงโครงสร้างและเชิงพลวัตของน้ำที่ถูกจำกัดในท่อที่มีโครงสร้างระดับนาโนเมตร ณ อุณหภูมิห้อง พบว่าน้ำที่มีความหนาแน่น 1 กรัมต่อลูกบาศก์เซนติเมตร เมื่ออยู่ในท่อนาโนทิวบ์ชนิด คาร์บอน และ โบรอนไนไตรด์ ที่มีผนังชั้นเดียวแบบอาร์มแชร์ จะมีโครงสร้างการกระจายตัวและความเร็วในการเคลื่อนที่ตามแนวท่อแตกต่างกันไป ขึ้นอยู่กับขนาดเส้นผ่าศูนย์กลางของนาโนทิวบ์ โดยน้ำที่อยู่ในท่อนาโนทิวบ์ชนิด (9,9)-อาร์มแชร์ จะมีการจัดเรียงตัวคล้ายท่อน้ำแข็งรูปทรงกระบอกหกเหลี่ยมและมีผนังเพียงชั้นเดียว ต่างจากที่พบในท่อนาโนทิวบ์ขนาดใหญ่ขึ้นซึ่งมีการจัดเรียงตัวในลักษณะเป็นท่อหลายชั้นและระหว่างชั้นเกิดการแลกเปลี่ยนโมเลกุลของน้ำได้อย่างอิสระ อันเป็นสาเหตุสำคัญทำให้การแพร่ตามแนวท่อนาโนทิวบ์ขนาดใหญ่ช้ากว่าท่อขนาดเล็ก นอกจากนี้ยังพบว่าการแพร่ของน้ำในท่อนาโนทิวบ์ขนาดเล็กชนิด โบรอนไนไตรด์ มีอัตราเร็วกว่าในท่อนาโนทิวบ์ชนิด คาร์บอน เนื่องจากมีแรง adhesive force ภายในท่อสูงกว่า

Abstract: Structure and dynamic properties of water confined in nanotubes were investigated by using a molecular dynamics (MD) technique. The water density of 1.00 g/cm^3 was placed inside the periodic models of the single-walled armchair carbon nanotubes (SWCNTs) and boron nitride nanotubes (SWBNNTs) at the average temperature of 298 K. It was found that the confinement effect of narrow-pore nanotubes has a strong influence on both the molecular distribution and transport phenomena. The six-membered ring structure of the single-walled ice-like nanotube was observed in the (9,9)-armchair SWCNT and SWBNNT, while a multi-layered cylindrical structure was predicted in the large-pore nanotubes. In the latter cases, the water molecules can freely exchange between layers. This, consequently, causes a significant reduction of an axial diffusion coefficient. In narrow-pore systems, water molecules permeate through the BNNTs faster than through the SWCNTs. This is due to a stronger adhesive force generated from the attractive water-nanotube interactions in the BNNT systems.

Introduction: The transport phenomena and molecular distribution of water confined in nanopores have become important aspects for attaining scientific and technological features in the biological micro-fluidic systems and the delivery of beneficial molecules such as drugs, genes and biomolecules to the target cells [1,2]. Carbon nanotubes (CNTs) have gained much attention as prototypes for biological water channels due to their simplicity, stability, and nanoporosity. However, their electrical neutrality impedes them to reproduce some important features of biological channels, in terms of irregular surfaces and highly inhomogeneous charge distributions. Boron nitride nanotubes (BNNTs), an isoelectronic structure of CNTs, have been found to exhibit many superior properties and offer substantial advantages over CNTs such as a high Young's modulus, thermal conductivity and resistance to oxidation [3]. Furthermore, an alternating combination of boron and nitrogen atoms in their structure may mimic some characteristics of biological water channels better than CNTs. Therefore, the research on structural and dynamic properties of water confined in single-walled boron nitride nanotubes (SWBNNTs) is also of interest. Here, we report molecular dynamics simulations of water in different diameters of SWCNTs and SWBNNTs. The distribution and diffusion of water confined in nanotubes are discussed.

Methodology: The molecular dynamics simulations were performed in the *NVT* ensemble at the average temperature of 298 K using a time step of 1 fs. Coordinates and velocities of atoms were stored every 50 fs of 1 ns after the equilibration period of 0.3 ns for the subsequent analysis. The self-diffusion coefficients were determined by using the Einstein relation. All simulations were executed by using the DL_POLY 2.0 program. The systems studied were periodic rigid models of the (*n*,*n*)-armchair SWCNTs and SWBNNTs of a fixed length of 36.89 Å. The (*n*,*n*)-armchair nanotubes were in series *n* = 9, 12, 14, 16, and 20 which correspond to the effective diameters of 8.86, 12.92, 15.62, 18.34 and 23.74 Å, respectively. These nanotubes were filled with a certain number of water molecules at a density of 1.0 g/cm^3. Water was described with the extended simple point charge (SPC/E) model [4], while the water-nanotube interactions were described by only a short-range Lennard-Jones potential with $\varepsilon =$ 0.1230, 0.1216, and 0.1502 kcal/mol for C-O, B-O, and N-O interactions, respectively, and $\sigma_{C\text{-}O} = \sigma_{B\text{-}O} = \sigma_{N\text{-}O} = 3.26$ Å.

Table 1. Axial self-diffusion coefficients ***D*** (cm^2/s) of water in SWCNTs and SWBNNTs at the average temperature of 298 K and the water density of 1.00 g/cm^3.

Model	***D*** (cm^2/s)	Model	***D*** (cm^2/s)
(9,9)-armchair SWCNT	67.88 x 10^{-5}	(9,9)-armchair SWBNNT	152.85 x 10^{-5}
(12,12)-armchair SWCNT	15.02 x 10^{-5}	(12,12)-armchair SWBNNT	21.79 x 10^{-5}
(14,14)-armchair SWCNT	7.65 x 10^{-5}	(14,14)-armchair SWBNNT	8.27 x 10^{-5}
(16,16)-armchair SWCNT	3.53 x 10^{-5}	(16,16)-armchair SWBNNT	4.23 x 10^{-5}
(20,20)-armchair SWCNT	1.68 x 10^{-5}	(20,20)-armchair SWBNNT	4.09 x 10^{-5}

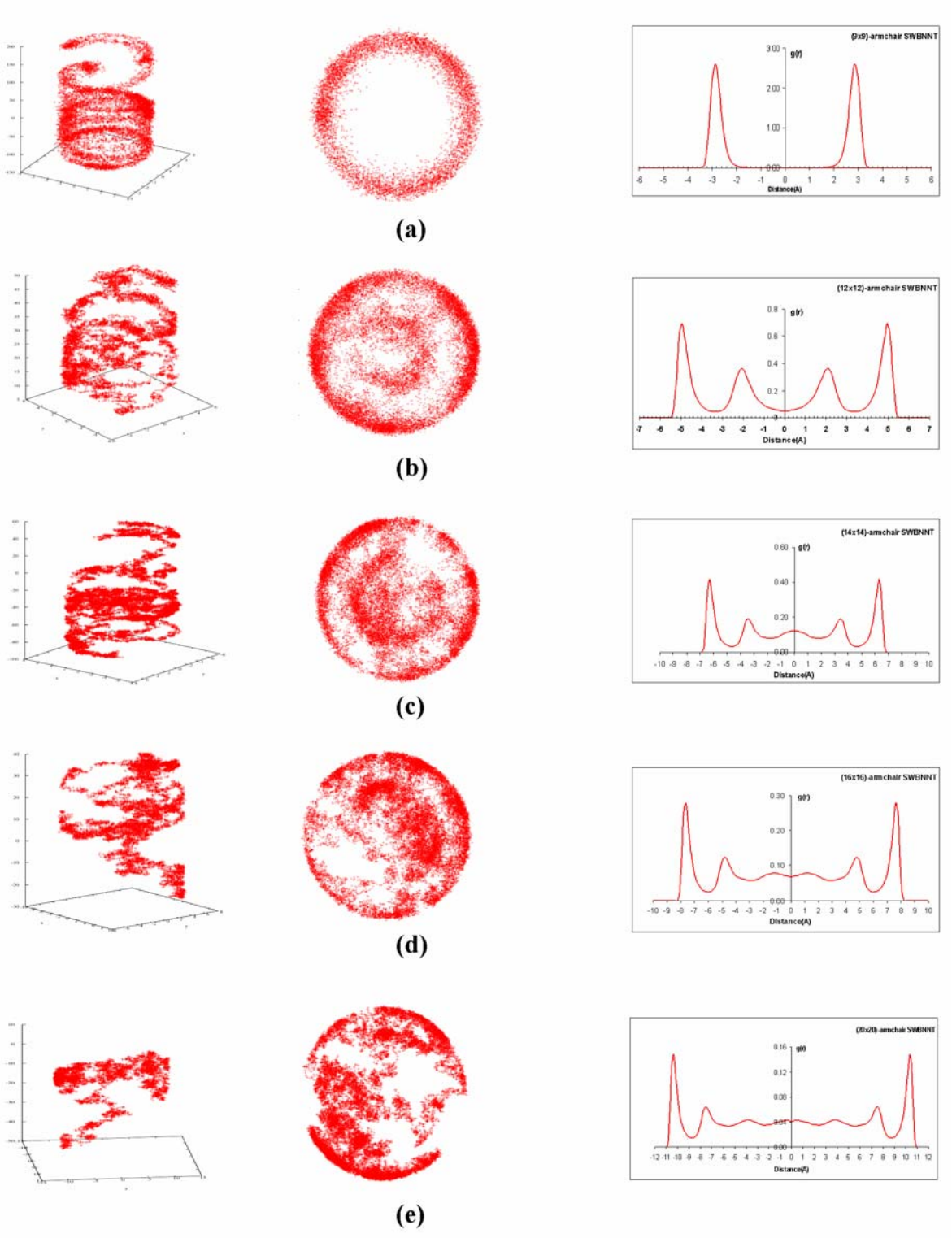

Figure 1. Three-dimensional trajectories (left) of a selected water molecule in (9,9)- (a), (12,12)- (b), (14,14)- (c), (16,16)- (d) and (20,20)- (e) armchair SWBNNTs; their

projections onto the *xy* plane (middle); and cylindrical $g(r)$ distribution functions of water with respect to the center of those SWBNNTs (right).

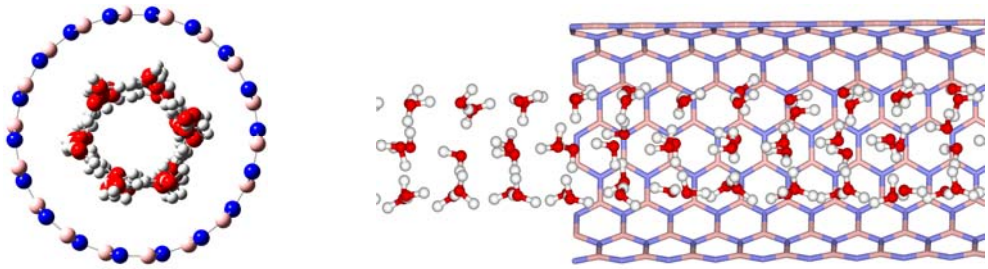

(a) **(b)**

Figure 2. Top view (a) and side view (b) of a snap short of the six-membered ring structure of the single-walled ice-like nanotube in a (9,9)-armchair SWBNNTs.

Results, Discussion and Conclusion: Dynamic properties of water confined in various nanotubes were expressed in terms of its self-diffusion coefficient along the nanotube axis. The self-diffusion coefficients of water in different diameters of both SWCNTs and SWBNNTs are listed in Table 1. In both types of nanotube, the calculated self-diffusion coefficient decreases as the nanotube diameter increases. This occurrence can be explained by tracing the molecular trajectory of water molecules throughout the simulation run. In the (9,9)-armchair nanotubes, the smallest diameter nanotube studied, the track picture of their trajectory resembles a circular helix (Figure 1a). Over this timescale, the motion of one water molecule is highly correlated with that of the neighbouring water molecules. As a result, they move together in the same direction along the nanotube length. Furthermore, the water in this narrow pore was conducted to form the six-membered ring structure of single-walled ice-like nanotube (Figure 2). The exchange of water molecules between adjacent positions is intractable, and thus the axial diffusion becomes forceful. In the larger diameter nanotubes, the multi-layered water nanotube is observed (Figures 1b-e). The resulting cylindrical $g(r)$ distribution functions (Figures 1b-e) of water with respect to the centre of the nanotubes show the non-zero minimum values of the function between neighbouring peaks, indicating that the exchange of water molecules between layers becomes possible. This results in the reduction of an axial self-diffusion coefficient in the large-pore nanotubes. Comparing between the same pore sizes of SWCNTs and SWBNNTs, it was found that the axial diffusion of water in the SWBNNTs is faster than that in the SWCNTs. This may be understood in terms of the adhesive force generated from the attractive interactions between water and nanotubes.

References:

(1) Liu, Y., Wang, Q., Zhang L., Wu, T. *J. Langmuir*. 2005. **21**, 12025-12030.
(2) Liu, Y., Wang, Q., Wu. T., Zhang L. *J. Chem. Phys*. 2005 **123**, 234701-234707.
(3) Won, C, Y., Aluru, N, R. *J. Am Chem. Soc*. 2007, **129**, 2748-2749.

(4) Lyubartsev, A. P., Laaksonen, A. *J. Phys. Chem.* 1996**, 100***,* 16410-16418.

Keywords: Water, Molecular dynamics (MD), Carbon nanotubes (CNTs), Boron Nitride nanotubes (BNNTs).

Acknowledgements: We gratefully acknowledge the Commission of Higher Education (CHE), the Graduate School Kasetsart University funds, Thailand Research Fund (TRF Senior Research Scholar to JL) and NANOTEC Center of Excellence at Kasetsart University for funding this research.

การศึกษาทางทฤษฎีของอิทธิพลของหมู่ เมทิล ฟีนิล ฟลูโอไรด์ และ ท่อคาร์บอนนาโน ที่แทนที่บนอะดีนีนต่อพันธะไฮโดรเจนของ คู่เบส อะดีนีน และไทมีน ในดีเอนเอ

THE INFLUENCE OF -CH_3, -C_6H_5, -F, AND –CNT ON THE HYDROGEN-BONDED ADENINE/THYMINE ADDUCT

มนตรี สว่างพฤกษ์[1,2], นงค์นุช อาจฤทธิ์[1,2], พิพัฒน์ คงประชา[1,2], จำรัส ลิ้มตระกูล[1,2,*]

Montree Sawangphruk[1,2], Nongnuch Artrith[1,2], Pipat Khongpracha[1,2], Jumras Limtrakul[1,2]
[1] Laboratory for Computational & Applied Chemistry, Department of Chemistry, Faculty of Science, Kasetsart University, Bangkok 10900, Thailand
[2] Center of Nanotechnology, Kasetsart University, Bangkok 10900, Thailand;
e-mail address: fscijrl@ku.ac.th (J. Limtrakul)

บทคัดย่อ: ศึกษาสมบัติเชิงโครงสร้างและพลังงานของคู่เบส อะดีนีน และไทมีน ในดีเอนเอ ที่ถูกแทนที่ด้วยหมู่ เมทิล ฟีนิล ฟลูโอไรด์ และท่อ คาร์บอนนาโน ด้วยระเบียบวิธีการคำนวณแบบ ONIOM(6-31G(d,p):AM1) พบว่าอิทธิพลของหมู่เมทิล ฟีนิล และ ท่อคาร์บอนนาโน มีผลต่อพลังงานและความยาวพันธะไฮโดรเจนของคู่เบส อะดีนีน และไทมีนในดีเอนเอน้อยกว่าอิทธิพลของหมู่ฟลูโอไรด์ ทั้งนี้เนื่องจากหมู่ เมทิล ฟีนิล และ ท่อคาร์บอนนาโน คือหมู่ที่ให้อิเล็กตรอนแก่โมเลกุลของอะดีนีนในขณะที่หมู่ฟลูโอไรด์เป็นหมู่ดึงอิเล็กตรอนจากโมเลกุลของอะดีนีน ส่วนอิทธิพลของการแทนที่ด้วยท่อคาร์บอนนาโน ตรงตำแหน่งด้านข้างและด้านปลายของท่อคาร์บอนนาโน พบว่าการแทนที่ที่ปลายท่อ ส่งผลให้พันธะไฮโดรเจนของคู่เบสมีความเสถียรมากขึ้นกว่าการแทนที่ตรงตำแหน่งด้านข้างนอกจากนั้นจากการวิเคราะห์การเปลี่ยนแปลงของประจุของอะตอมภายในโมเลกุลยังให้ผลสอดคล้องกับการเปลี่ยนแปลงทางโครงสร้างและพลังงาน

Abstract: The geometries and energies of base pairs of T:A-COR are calculated at B3LYP/6-31G(d,p) level for R=CH_3, C_6H_5 and F and at ONIOM(B3LYP/6-31G(d,p):AM1) level for R= Carbon Nanotubes. Frontier molecular orbital (FMO) analysis and natural bond orbital (NBO) analysis have been carried out on the optimized geometries. The charge distribution and bonding analysis have also been investigated. The results show that the stabilization energy decreases when the –COR groups are substituted at the reactive amino group of adenine via peptide bond. The NBO analysis shows the charge transfer between the two monomers of the A:T base pair derivatives. The decrease in the hydrogen bond strength is correlated with the substituting groups.

Introduction: Since Iijima discovered carbon nanotubes (CNTs) in 1991, these materials have fascinated a myriad of investigators for their distinct structural, electrical, mechanical, and electromechanical properties. The use of nanotubes in biological applications is one of the most important applications, such as artificial muscles (actuators), nanotube field-effect transistors, nanotube-DNA electrochemical sensors and biomedical sensors. The concept of using DNA to direct the assembly of nanotubes into nanoscale devices is also attracting attention because of its potential to assemble a multicomponent system in one step by using different base sequences for each component. So far, the focus in this area has been on placing DNA at the tips and the side walls of nanotubes. To produce reactive sites to which the DNA may be attached, the nanotubes are mainly oxidized by nitric acid (HNO_3) treatment to introduce carboxyl groups on their tips; this procedure also introduces carboxyl groups at the sidewalls. DNA molecules with functional linkers are then coupled to the carboxyl groups on the nanotubes. In this work, to know the effect of CNTs to the hydrogen bonds on the A:T base pair of DNA, peptide bond is constructed by using the acid-base reaction between adenine and a carboxylic group of carbon nanotubes. This reaction is focused only on the reactive site of adenine that is the secondary amino (NH9) of adenine,

like the reaction between adenine and deoxyribose in the DNA formation. To understand the effect of the substuents to the hydrogen bonds on the A:T base pair, we have constructed the model, T:ACOR where R are CH_3, C_6H_5, F, tip-CNT and side-CNT.

Methodology: The geometries and energies of base pairs of T:A-COR are calculated by using the GAUSSIAN 03 program at B3LYP/6-31G(d,p) level for R = CH_3, C_6H_5 and F and at the ONIOM(B3LYP/6-31G(d,p):AM1) level for R = carbon nanotubes. The counter poise correction method was used to correct the basis set superposition error (BSSE) for all binding energies portrayed in this work. The T:ACO-nanotubes were taken and are represented in Figure 1, in which the high-level part contains 16 carbon atoms (see the ball and stick atoms in Figure 1). Such an ONIOM (B3LYP/6-31G (d,p):AM1) approach and a modeling scheme were utilized in our previous study of the Diels Alder cycloadditions of single-wall carbon nanotubes with electron-rich dienes. A similar ONIOM model was used in other groups in the theoretical studies of carbon nanotubes, such as the base-catalyzed [2,3] cycloaddition of transition metal oxide (OsO_4) on [5,5] SWNT and the 1,3-dipolar cycloaddition onto the sidewalls of [5,5] SWNT. At the same time, frontier molecular orbital (FMO) analysis and natural bond orbital (NBO) analysis have been carried out on the optimized geometries. The charge distribution and bonding analysis have also been investigated.

Results, Discussion and Conclusion: It was found that two calculated hydrogen bond lengths in A:T are 2.94 and 2.84 Å, which approach to 2.95 and 2.82 Å of X-ray. On the other hand, the BSSE-corrected energy of A:T is -12.35 kcal/mol, which is in reasonable agreement with -12.10 kcal/mol of the experimental value. These suggest that the results of DFT calculation at B3LYP/6-31G(d,p) level is comparable with the experimental X-ray crystallography data. In case of ($COCH_3$)-A:T and (COC_6H_5)-A:T, both methyl and benzyl groups are the slight electron donating groups, which lead to the similar result of -12.70 kcal/mol of relative energies. The (COF)-A:T is, in contrast, more exothermic than ($COCH_3$)-A:T and (COC_6H_5)-A:T because the fluoride group is the strong electron withdrawing group. For (9-carbonyl tip-[5, 5]-SWNT)-A:T and (9-carbonyl sidewall-[5, 5]-SWNT)-A:T, we found that the former complex gives -12.34 kcal/mol of corrected energy and the latter complex provides -11.64 kcal/mol of corrected energy. This is due to the effect of electron delocalize existing only in case of (9-carbonyl tip-[5, 5]-SWNT)-A. FMO and NBO analyses have, in addition, confirmed the alteration of structures and energies (see Figure 1 and Table 1).

Table 1 Bond lengths (pm) of base pairs optimized at ONIOM(B3LYP/6-1G(d,p):AM1).

Models	Bond lengths (pm)					
	O4'-N6	O4'-H6	N6-H6	N1-N3'	N1-H3'	N3'-H3'
A:T	294.0**(1)**	192.1**(1)**	102.2**(5)**	284.5**(6)**	179.7**(6)**	104.9**(1)**
($COCH_3$)-A:T	293.0**(4)**	191.0**(4)**	102.3**(2)**	285.7**(3)**	181.1**(3)**	104.6**(4)**
(COC_6H_5)-A:T	293.3**(3)**	191.3**(3)**	102.3**(2)**	285.3**(5)**	180.6**(5)**	104.7**(2)**
(COF)-A:T	291.9**(6)**	189.8**(6)**	102.4**(1)**	286.6**(1)**	182.2**(1)**	104.4**(6)**
(CO-side-SWNT)-A:T	293.5**(2)**	191.6**(2)**	102.2**(5)**	285.6**(4)**	181.0**(4)**	104.7**(2)**
(CO-tip-SWNT)-A:T	292.8**(5)**	190.7**(5)**	102.3**(2)**	285.9**(2)**	181.4**(2)**	104.6**(4)**

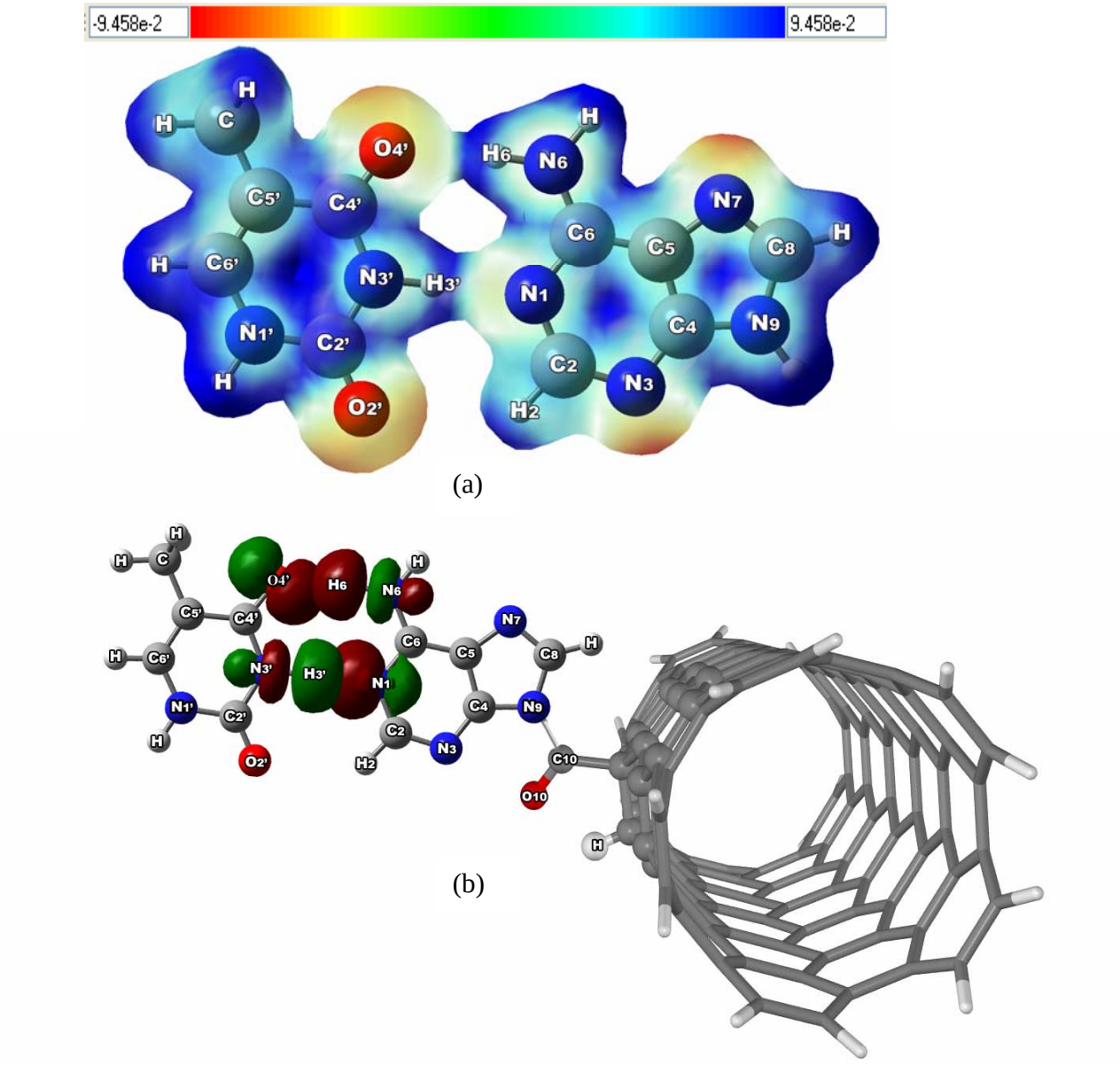

Figure 1 (a) The electrostatic potential is mapped onto a particular value of the total SCF electron density of A:T base pair.

(b) Orbital interaction of (RCO)-A:T where R is a sidewall SWNT.

References:

(1) Sumio Iijima (1991) *Nature*, **354**, 56-58.
(2) Richard E. Smalley (1998) *Nature*, **391**, 59-62.
(3) Supawadee Namuangruk, Piboon Pantu and Jumras Limtrakul (2004) *Journal of Catalysis*, **225**, 523-530.
(4) Supawadee Namuangruk, Piboon Pantu and Jumras Limtrakul (2005) *Journal of Chemical Physics and Physical Chemistry*, **6**, 1333-1339.
(5) Chompunuch Warakulwit, Suwassa Bumrungsap, Pataraporn Luksirikul, Pipat Khongpracha and Jumras Limtrakul (2005) *Studies in Surface Science and Catalysis*, **156**, 823-828.

Keywords: Carbon nanotubes, Base pairs, A:T.